



Seismic Performance of RC Frame Buildings with Decoupled Infills

Donatello Cardone, Viggiani Luciano Rocco Salvatore, Milijaš Aleksa, Šakić Bogdan, Marinković Marko & Butenweg Christop

To cite this article: Donatello Cardone, Viggiani Luciano Rocco Salvatore, Milijaš Aleksa, Šakić Bogdan, Marinković Marko & Butenweg Christop (06 Feb 2025): Seismic Performance of RC Frame Buildings with Decoupled Infills, Journal of Earthquake Engineering, DOI: [10.1080/13632469.2025.2459787](https://doi.org/10.1080/13632469.2025.2459787)

To link to this article: <https://doi.org/10.1080/13632469.2025.2459787>



Published online: 06 Feb 2025.



Submit your article to this journal [↗](#)



View related articles [↗](#)



View Crossmark data [↗](#)



Seismic Performance of RC Frame Buildings with Decoupled Infills

Donatello Cardone^a, Viggiani Luciano Rocco Salvatore^a, Milijaš Aleksa^b, Šakić Bogdan^b, Marinković Marko^{b,c}, and Butenweg Christop^b

^aDepartment of Engineering, University of Basilicata, Potenza, Italy; ^bCenter for Wind and Earthquake Engineering, RWTH Aachen University, Aachen, Germany; ^cFaculty of Civil Engineering, University of Belgrade, Belgrade, Serbia

ABSTRACT

Decoupled infills have been recently proposed to improve the seismic performance of infilled RC frame buildings. In this paper, the so-called INODIS system, developed at the RWTH Aachen University, is investigated. The INODIS system exploits soft elastomeric material to decouple masonry infills from the surrounding frame, while withstanding OOP loads through a suitable mechanism. A typical 6-storey RC frame building equipped with, alternatively, traditional and decoupled infills is examined through Nonlinear response-time history analyses, considering IP/OOP interaction for the infills. The results of this study clearly confirm the good seismic performance and significant damage reduction achievable with decoupled infills.

ARTICLE HISTORY

Received 2 March 2024
Accepted 11 January 2025

KEYWORDS

Masonry infills; RC frame buildings in-plane behavior; out-of-plane behavior; decoupled infills; seismic performance

1. Introduction

Unreinforced masonry (URM) infills are widely used in Reinforced Concrete (RC) frame buildings, due to their good mechanical and thermal properties. URM infills are usually considered as non-structural elements (Taghavi and Miranda 2002; Villaverde 1997) and are neglected in the seismic design of the building. However, results of previous research clearly point out that the presence of URM infills can significantly affect the structural strength and stiffness of the building (Asteris et al. 2015; Hak, Morandi, and Magenes 2017; Ricci, Verderame, and Manfredi 2011) and modify the inelastic mechanism of the structure. Seismic damage to infills can produce considerable losses and dramatic consequences as observed in past earthquakes, e.g. L'Aquila 2009, (Braga et al. 2011), Lorca 2011 (Hermanns et al. 2014), Central Italy 2016 (Perrone et al. 2019), Albania 2019 and (Marinković et al. 2022).

Extensive damage to masonry infills can jeopardize the usability and immediate occupancy of the building after an earthquake with obvious important socio-economic consequences, including large economic losses for building repair (Cardone and Perrone 2017). Although several methods are available for estimating seismic losses in RC buildings with infill walls (Del Gaudio, De Risi, and Verderame 2021; Rossi, Morandi, and Magenes 2021), the influence of variability and uncertainty in the infill properties can make the seismic loss assessment of RC buildings quite difficult (Mucedero, Perrone, and Monteiro 2022, 2023).

Moreover, the strong interaction between masonry infills and RC frame can trigger brittle shear failure of RC columns (Milanesi, Morandi, and Magenes 2018; Tasligedik 2014). In-Plane (IP) and Out-Of-Plane (OOP) failure are the main failure modes observed in URM walls during seismic events. Both are characterized by degradation of strength and stiffness and low energy dissipation (Priestley 1985).

Recent studies (Gesualdi, Viggiani, and Cardone 2020) emphasised the relevance of the IP/OOP interaction, showing that the collapse of masonry infills can significantly affect the life-safety seismic performance of RC buildings, threatening human life either inside or outside the building.

For these reasons, in the last years, different solutions for the improvement of the seismic behaviour of masonry infills and partitions have been proposed. A number of solutions are based on the idea of increasing load-bearing capacity of masonry infills rigidly connected them to the RC frame. For instance, this can be achieved by adding reinforcing bars in the bed joints (Da Porto et al. 2013; Vintzileou, Adami, and Palieraki 2016), or by placing steel grid reinforcement on the lateral surfaces of the wall (Calvi and Bolognini 2001) or by using plaster reinforcement with textile meshes (Akhoundi et al. 2018; Valluzzi et al. 2014). However, the high installation costs could limit the use of these solutions in common practice. Additionally, reinforced/strengthened masonry infills must be considered as load-bearing elements which require appropriate design.

An alternative approach could be that of increasing the deformation capacity of masonry infill walls by using different types of sliding materials (Di Trapani et al. 2020; Morandi, Milanese, and Magenes 2018; Preti and Bolis 2017; Verlato et al. 2016). Some authors (Huang et al. 2024; Zhang et al. 2022) argued that the main critical point of this approach could be the quality of production and installation of sliding surfaces, which may significantly affect the effectiveness of the system, especially in the long run.

Recently, another solution has been proposed which relies on the deformability of elastomeric material. The INODIS (INnOvative Decoupled Infill) System (Marinković and Butenweg 2019) increases the IP and OOP displacement capacity of URM infills by means of dissipative/deformable connections placed along the contact areas between the infill (partition) and the surrounding RC frame. The efficiency of the INODIS system has been assessed through full-scale experimental tests on 1-storey, 1-bay experimental mock-up (Marinković and Butenweg 2022).

In this paper, the seismic response of a building model with decoupled infills (with INODIS) is examined through non-linear response-time history analyses. The numerical model previously implemented in Opensees by (Gesualdi, Viggiani, and Cardone 2020) is further developed and calibrated to capture the IP/OOP behaviour of decoupled infills. By means of this model, seismic performance and expected losses of the building model, for different earthquake intensity levels, are evaluated, comparing traditional and innovative (INODIS) solutions for masonry infills.

2. INODIS System

Motivation for the development of the INODIS system is a lack of available cost-effective solutions that can successfully reduce the seismic damage in masonry infill walls. The proposed INODIS system is based on the concept of decoupling of a masonry infill from the surrounding RC frame. [Figure 1](#) shows masonry infill installed with INODIS system. At the top of the infill wall and along the vertical edges U-shaped elastomers are placed around plastic bars which are previously attached to the surrounding RC frame. First layer of U-shaped bearings is made of soft elastomeric material which allows later activation of masonry infills under in-plane deformation of RC frame. Moreover, sliding surfaces are glued on the plastic profiles, concrete and U-shaped elastomer in order to reduce the friction effects and provide sliding between masonry infill and RC frame. The second layer of U-shaped profile is made of stiffer elastomer. In combination with plastic bar attached to the surrounding frame, U-shaped elastomers represent the shear key for the wall in the OOP direction and thus prevent the OOP movement of the wall. At the bottom of the infill wall decoupling is achieved by three stiffer elastomer strips. The middle strip is glued to the bottom beam, while outer strips are glued to the infill wall. In this way shear key effect is provided at the bottom too.

The additional advantage of INODIS system is that it can be easily modified for different levels of seismic events by varying thickness and stiffness of elastomers. Therefore, INODIS system can successfully provide high levels of seismic safety to various configurations of masonry infills subjected to combined in-plane and out-of-plane actions.

The INODIS system has been developed through a series of national and European projects from 2013 to 2024, and its effective earthquake protection has been demonstrated by extensive quasi-static cyclic and dynamic (shaking table) experimental tests on typical wall configurations, both with and without openings (e.g. doors and windows). Recently, the INODIS system

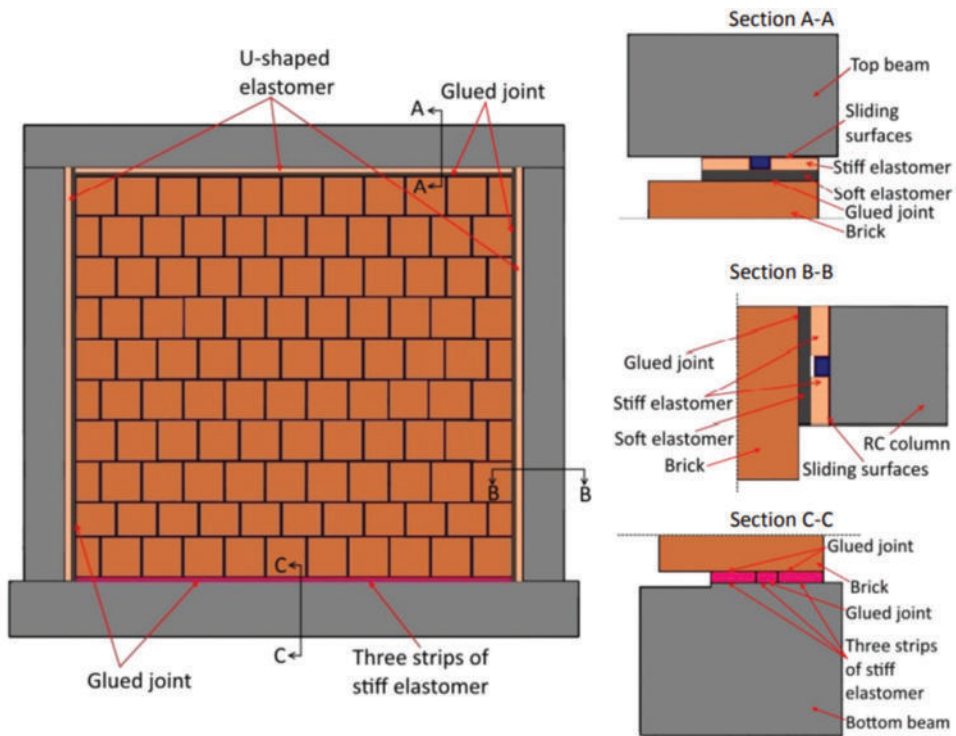


Figure 1. INODIS decoupling system (Marinković and Butenweg 2019).

has been patented and started to be marketed by REGUPOL GMBH (see <https://acoustics.regupol.com/products/regupol-inodis/>).

3. Methodology of the Study

The influence of the IP/OOP interaction of URM walls on the seismic response of RC frame buildings is investigated following a four steps methodology: (i) Step 1: Selection of case-study, Modeling assumptions, Ground motion selection; (ii) Step 2: Definition of seismic Performance Levels (PLs); (iii) Step 3: Non-linear response-Time History Analyses (NTHA); (iv) Step 4: Assessment of non-structural damage.

The basic idea of this study is to compare the seismic response of an existing building with traditional infills with that of the same building with decoupled infills (with INODIS). From a theoretical point of view, this could be the case where the original infills are replaced (e.g. because extensively damaged by a previous earthquake) by new infills equipped with the INODIS system. In this case, however, some problems may arise: removing masonry infills means, most of the times, replacing electrical and plumbing systems. Therefore, from a practical point of view, it is appropriate to stress on the future changes that engineers should make by using new solutions instead of traditional ones for the design of new infilled reinforced concrete frame buildings.

3.1. Case-Study Building and Ground Motion Selection

A six-storeys RC frame building representative of typical multi-storey residential buildings realized in Italy in the '90s (see Fig. 2) is selected. The building features an in-plane rectangular shape with 21.40

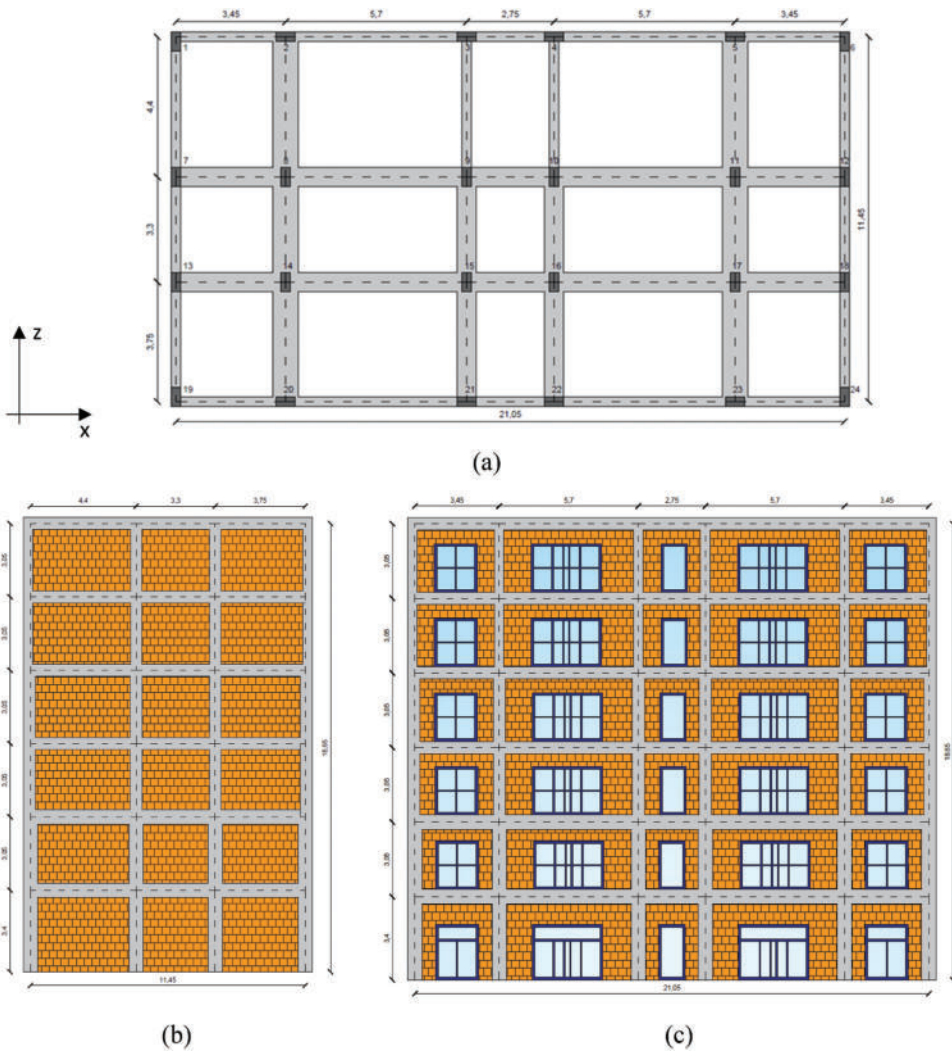


Figure 2. Case Study: (a) floor plan; (b) Short side elevation; (c) Long side elevation.

m by 11.80 m dimensions, 3.40 m interstorey height for the first level and 3.05 m for the upper ones. The building has five frames in the long direction (X-dir. In Fig. 2) and three external frames in the short direction (Z-dir. In Fig. 2). RC columns taper in both directions passing from the second to the third floor and then again from the fourth to the fifth floor. In the Z-dir., a dog-leg stair with cantilever steps is sustained by two stiff “knee” beams. Structural characteristics (geometric dimensions, reinforcement ratios, structural details, etc.) are derived from a simulated seismic design, according to the standards and state of practice enforced in Italy before ’90s (Ministerial Decree DM March 3, 1975 and the decrees that followed DM June 19, 1984 and DM June 24, 1986). A concrete compressive strength of 25 MPa and a steel yield strength of 430 MPa (FeB44K deformed steel rebars) are considered. More details on the dimensions and steel reinforcement of beam and columns sections can be found in (Gesualdi, Viggiani, and Cardone 2020).

URM infill walls realized with hollow clay bricks arranged in two single layers (150 + 80 mm thickness), separated by an air-cavity, are considered (see Fig. 3(a)). The URM infills feature large openings in the X-direction (equal, on average, to 40%), while there are no openings in the

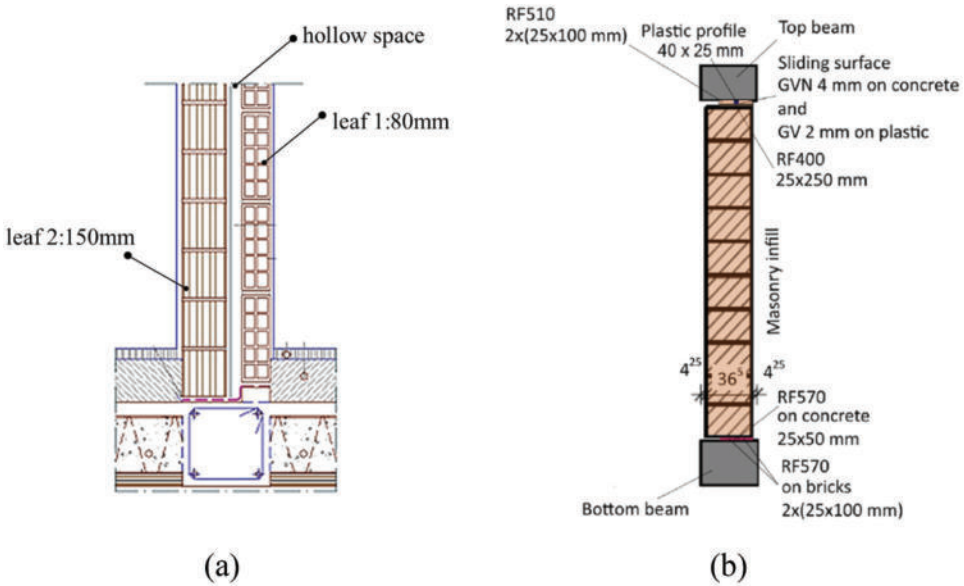


Figure 3. Types of infill considered: (a) Double layer infills and (b) Modern single layer infills with INODIS system (Marinković and Butenweg 2019).

Z-direction. A retrofit intervention aimed at replacing the original double-layers infills with modern single-layer (365 mm thickness) infills equipped with the INODIS system (see Fig. 3(b)) is then considered.

The case-study building is supposed to be located in the city of L'Aquila (central Italy) on soil type C (soft soil). The aforesaid site and soil conditions are purposely selected to investigate the seismic performance of the building for the highest levels of seismic hazard expected in Italy. Three different earthquake intensity levels, with return periods equal to 50 years (≈ 0.156 g PGA on soil type C), 500 (≈ 0.347 g PGA on soil type C) and 2500 (≈ 0.467 g PGA on soil type C) are selected for NTHA. The conditioning Intensity Measure (IM) for the record selection is the 5%-damping spectral pseudo-acceleration $S_a(T^*)$ at the fundamental period of vibration T^* . In this study T^* was assumed equal to 0.5 s for the model with traditional infill and 1.0 sec for the model with decoupled infills, based on results from modal analysis (see Table 2). For each seismic intensity, a set of twenty natural ground motion pairs, compatible with suitable Conditional Mean Spectra, derived considering the M-R- ϵ (Magnitude-Distance-Deviation) disaggregation and a proper attenuation relationship for the city of L'Aquila, is used. As an example, Fig. 4 shows the spectra of 20 pairs of records for L'Aquila, soil type C, conditioned to $S_a(T^* = 1 \text{ sec}) = 0.365$ g, which corresponds to the spectral acceleration with 500 years return period.

3.2. Numerical Model

The seismic behaviour of the selected case-study building is described through a refined 3D nonlinear model implemented in OpenSees (McKenna 2011). A lumped plasticity model is adopted for RC beams and columns. The structural model also includes the staircase structure featuring inclined beams and cantilever steps. The model by Ibarra-Medina-Krawinkler (Ibarra and Krawinkler 2005; Ibarra, Medina, and Krawinkler 2005), implemented in OpenSees (McKenna 2011) as modIMKmodel, is selected to describe the cyclic degrading behaviour of plastic hinges of RC beams and columns. Possible shear failure (before or after flexural yielding) is taken into account in the model. To this end, all the hinges are pre-qualified

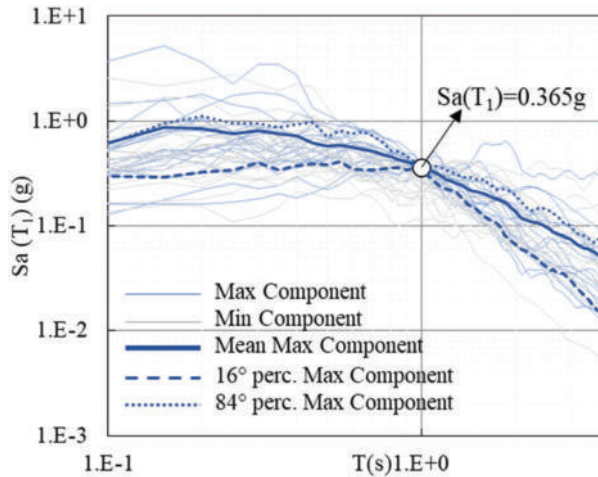


Figure 4. Response spectra of both horizontal components of the selected records for the case of L'Aquila, Soil Type C, with return period 500 years.

either as (i) ductile (shear failure does not occur: the moment-rotation skeleton curve is not modified), or (ii) shear critical (shear failure is expected for a given level of displacement (hence rotation): the moment-rotation skeleton curve is modified beyond the critical rotation by a softening branch whose slope is derived from the empirical formulation reported in (Aslani and Miranda 2005). More details about this collapse criterion can be found in (Ricci et al. 2019).

Concerning beam-column joints, a scissors model is adopted. In the scissor model, joint shear deformation is simulated by a rotational spring with degrading hysteresis. The element is implemented in OpenSees by defining two nodes, node “i” (master) and node “j” (slave), with the same coordinates at the centre of the joint (intersection of beam and column centrelines); the element connectivity is set such that node “i” is connected to the column by a rigid link and node “j” is connected to the beam by a rigid link. Next, a Zero-length rotational spring is used to connect the two nodes so that the column rigid link is connected to one end of the spring while the beam rigid link is connected to the other. More details on the calibration of the joint models can be found in (Di Domenico et al. 2022).

In this paper the attention is focused on the description of the mechanical behaviour of masonry infills, as they can strongly affect the seismic response of older RC frame buildings (featuring double-layers masonry walls with high slenderness ratio and weak beam-column joints without adequate shear reinforcement), triggering local failure mechanisms and threatening human life in case of the out-of-plane collapse.

Figure 5(a) shows the modelling strategy adopted for the infills. Each infill is described by means of two couples of no-tension struts (one for each direction). Therefore, the IP force levels in each strut are taken equal to 50% of the total. This modelling choice is adopted to better capture the transfer of shear stresses from the infill to the adjacent column.

The OOP behaviour of the infills is incorporated in the model, following the strategy first proposed by (Ricci et al., 2018a). More precisely, each strut has a central node connected to a geometrically coincident node, provided with lumped mass in the OOP direction. Since four struts are adopted for each wall (two parallel struts for each inclined direction), four out-of-plane masses and four sets of force-displacement curves are defined in the model for each wall (each representing one-fourth of the total mass or force response of the wall).

Zero-length nonlinear springs are inserted between these two nodes to reproduce the OOP force-displacement behaviour (see Fig. 5(b)). Trilinear force-displacement curves are adopted both for the undamaged and damaged OOP curves. The IP/OOP interaction is modelled by

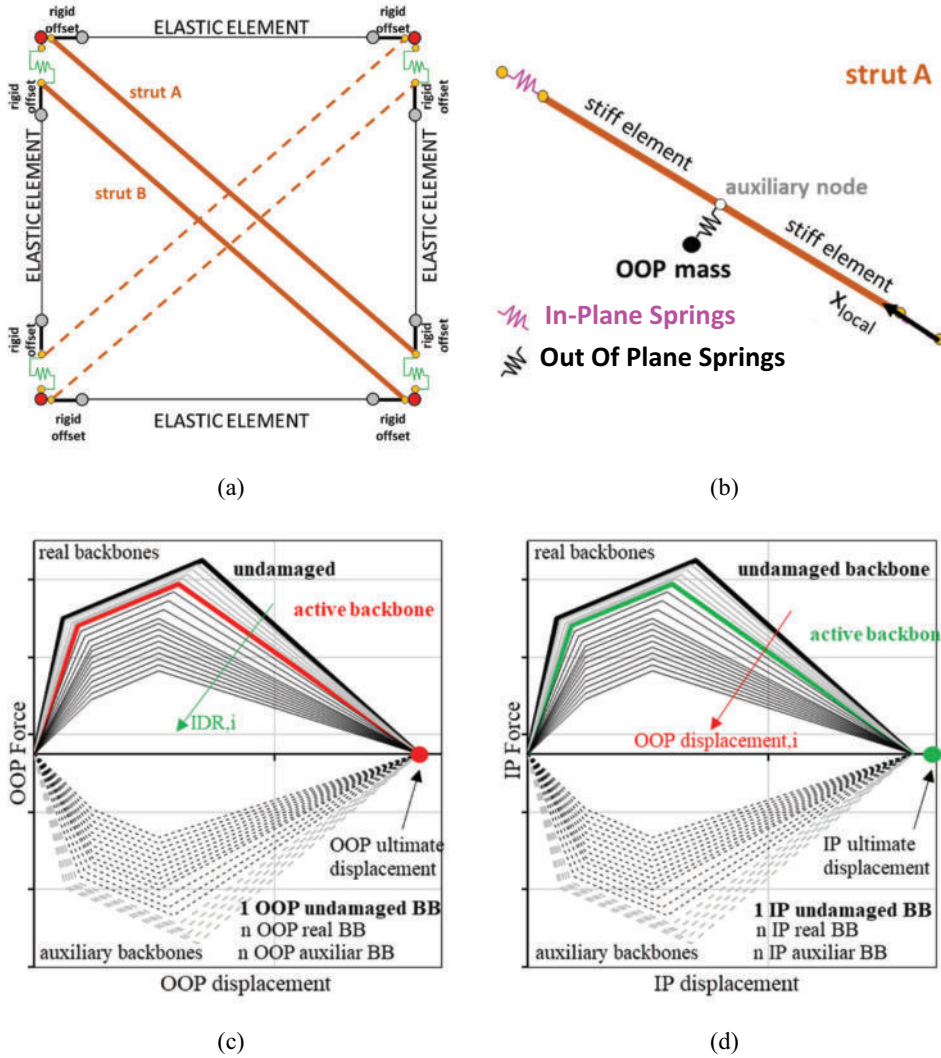


Figure 5. (a) Lumped plasticity macro model adopted for infills; (b) Close up view of each strut; (c) Real and auxiliary OOP curves to simulate the IP-OOP interaction (after Ricci, Di Domenico, and Verderame 2018b); (d) Real and auxiliary IP curves to simulate the IP-OOP interaction (after Ricci, Di Domenico, and Verderame 2018b).

means of a number of auxiliary springs (hence force-displacement curves) that mutually-neutralize (or activate) themselves based on the displacement demands recorded during the nonlinear time-history analysis (see Fig. 5(c,d)). In particular, the OOP strength/stiffness degradation is governed by the corresponding maximum interstorey drift level in the frame; Similarly, the IP strength/stiffness degradation depends on the maximum OOP displacements recorded. When either the IP or the OOP ultimate displacement of a generic leaf is reached, that leaf is automatically removed by the algorithm.

The IP behaviour of masonry infills is modelled following an equivalent compression-only strut approach. The effect of the openings on the IP force-displacement curves has been taken into account by suitable strength/stiffness reduction factors, derived with the formula proposed in (Decanini, Liberatore, and Mollaioli 2014).

The undamaged IP behavior of the infills has been modeled using the bilinear skeleton curve proposed in Sassun et al. (2016), assuming a compressive strength in the vertical direction (f_{mv}) of 1.2

MPa, a shear strength (τ) of 0.3 MPa, and an elastic modulus in the vertical direction (E_{mv}) of 1050 MPa, respectively, in accordance with Decanini et al. (2004). Moreover, a compression strength in the horizontal direction (f_{mh}) equal to 2.6 MPa and an elastic modulus in the horizontal direction (E_{mh}) of 1960 MPa have been assumed. Figure 6 shows some typical IP undamaged skeleton curves of double-layer traditional infills (a) with and (b) without openings.

The IP behaviour of the decoupled infills with INODIS is modelled by fitting available experimental results. Experimental curves in Fig. 7(a) represent envelopes obtained from the in-plane loading phase of the experimental tests on 1-storey, 1-bay frame with decoupled infills (referred to as DIO test in

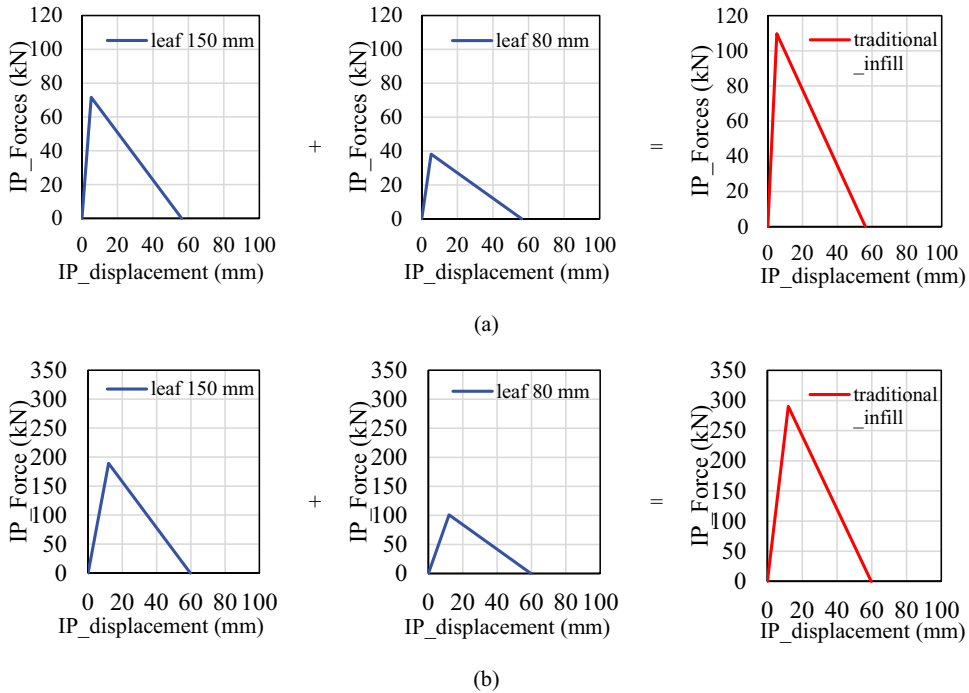


Figure 6. IP undamaged skeleton curves of double-layer traditional infills (a) With and (b) Without openings.

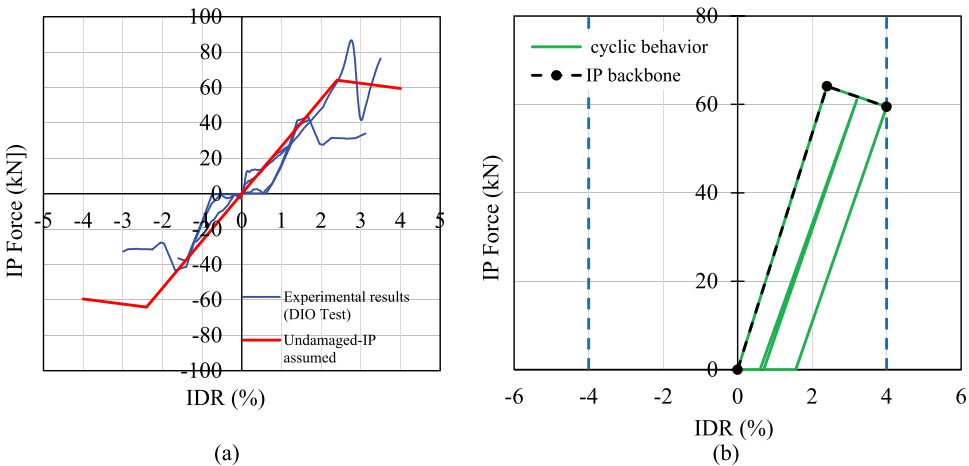


Figure 7. (a) Comparison between numerical and experimental IP skeleton curve and (b) Schematic cyclic behaviour of decoupled infills with INODIS.

Marinković and Butenweg 2019). In Fig. 7(a) two experimental curves can be noted. The first curve (with initial stiffness) refers to the first test on the as-built specimen while the second curve (with initial gap) refers to the test repeated on the same specimen. Both curves represent the contribution of the infill only derived from that of the infilled frame by subtracting the behavior of the RC frame. Four stages can be observed experimentally: (i) the initial long-lasting elastic behavior of the de-coupled infill due to the deformation of the surrounding U-shaped elastomeric layers, (ii) the damage of masonry infill due to crack opening, pointed out by drop in the lateral force in the first loading cycle for IDR of the order of 2.8%, (iii) the re-loading of the infill for IDR of the order of 0.6% followed by (iv) the attainment of a significant residual strength (about 50% the peak strength) due to the soft contact between infill and RC frame provided by the elastomers. There is no evidence of further damage on decoupled infills up to IDR of the order of 3% (see Fig. 7(a)).

In the numerical model the initial gap (phase (i)) has been neglected. Moreover, the peak force has been set at 2.4% IDR considering uncertainties related to the limited number of tests performed. A negative stiffness has been assumed for the post-peak branch of the curve up to 4% IDR (the highest value attained in the tests). However, the onset of significant IP damage was assumed to occur at 3% IDR. This is consistent with the experimental evidence and also compatible with results of previous studies on older RC frames. According to (Rossetto and Elnashai 2003), indeed, older RC frame buildings with substandard seismic details experience extensive damage for maximum interstorey drifts larger than 3%. It is then clear that this can affect the set-up and linking system of decoupled infills, as a result of the significant damage experienced by the surrounding RC members (e.g. for drift larger than 3% actions may be needed to restore the panel in its original position and replace some connections).

Experimental results (Marinković and Butenweg 2019) show that, for infills equipped with INODIS, the OOP behaviour does not affect significantly the IP behaviour under combined IP/OOP loading. Hence, it is assumed that damaged IP curves coincide with the undamaged IP curve (see Fig. 7(b)).

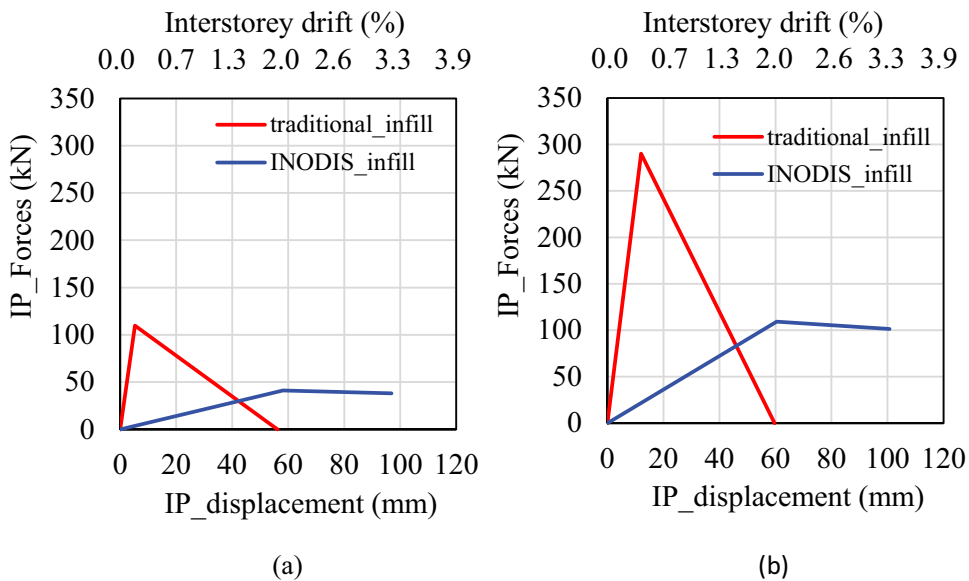


Figure 8. IP behaviour of traditional vs decoupled infills (with INODIS system) with (a) and without (b) openings.

The cyclic behaviour of both traditional and decoupled infills is described using the Uniaxial Material Hysteretic model of OpenSees (McKenna 2011), whose cyclic behaviour (for a typical decoupled infill with INODIS) is shown in Fig. 7(b).

Figure 8 compares the IP backbone curves of a traditional infill (with and without openings), located at the first storey of the building in the (a) long and (b) short direction, with those of the corresponding decoupled infill with INODIS. Decoupled infills show significantly lower lateral stiffness than the traditional infills, due to the deformability of the elastomeric material, and an apparent post-peak “ductile” behaviour, due to sliding between elastomer and RC surfaces (Fig. 1).

The out-of-plane behaviour of traditional infill walls is described by means of the relationships proposed in (Ricci et al. 2018b) and subsequently updated by (Di Domenico, Ricci, and Verderame 2021). The trilinear force-displacement skeleton curves are implemented in OpenSees (McKenna 2011) through the Uniaxial Hysteretic Material. The ultimate out-of-plane displacement of the panel is heuristically assumed to be 0.8 times the thickness of the panel.

For traditional infills, the IP/OOP interaction rule has been defined based on the semi-empirical relationships derived by (Ricci et al. 2018a, 2018b).

For decoupled infills with INODIS system, the OOP damaged/undamaged skeleton curves have been derived based on the results of the experimental tests reported in (Marinković and Butenweg 2019). Figure 9 compares the experimental curves derived from loading-unloading tests (Marinković and Butenweg 2019) with the skeleton curves implemented in the numerical model using the Uniaxial Material Hysteretic rule available in OpenSees (McKenna 2011). As can be seen, the numerical curves reproduce rather well the initial stiffness, first cracking, peak force and maximum displacement capacity observed experimentally. The degradation rate is set heuristically to capture the maximum lateral strength observed in the experimental tests while increasing the displacement amplitude.

Totally, one undamaged (black thick line in Fig. 5) plus 19 damaged skeleton curves (grey thin lines in Fig. 5) have been defined, covering a range of drift values ranging from 0 to 4%.

The cyclic degrading parameters of the OOP model were defined based on previous studies. In particular, the parameters governing the shape of the cycles for the Uniaxial Hysteretic Material are: (i) β , which controls the stiffness degradation during unloading, (ii) PinchX and PinchY, which control the pinching effect. These parameters were calibrated by Noh et al. (2017) by comparing numerical and experimental results for infilled RC frames. The values thus obtained are: 0.1, 0.9 and 0.1 for β , PinchX and PinchY, respectively. The cyclic behaviour thus obtained is shown in Fig. 10(a). For more

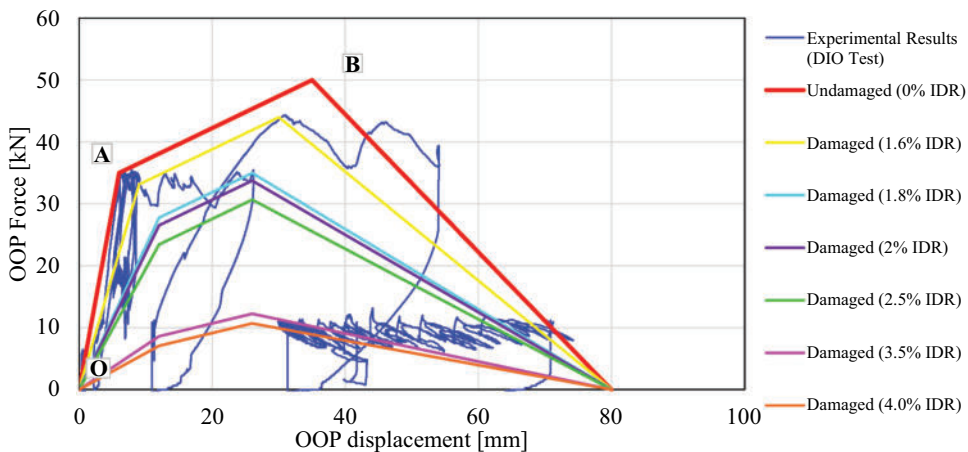


Figure 9. Comparison between experimental OOP cyclic behavior during combined IP/OOP tests and degrading OOP backbone curves assumed in the numerical model.

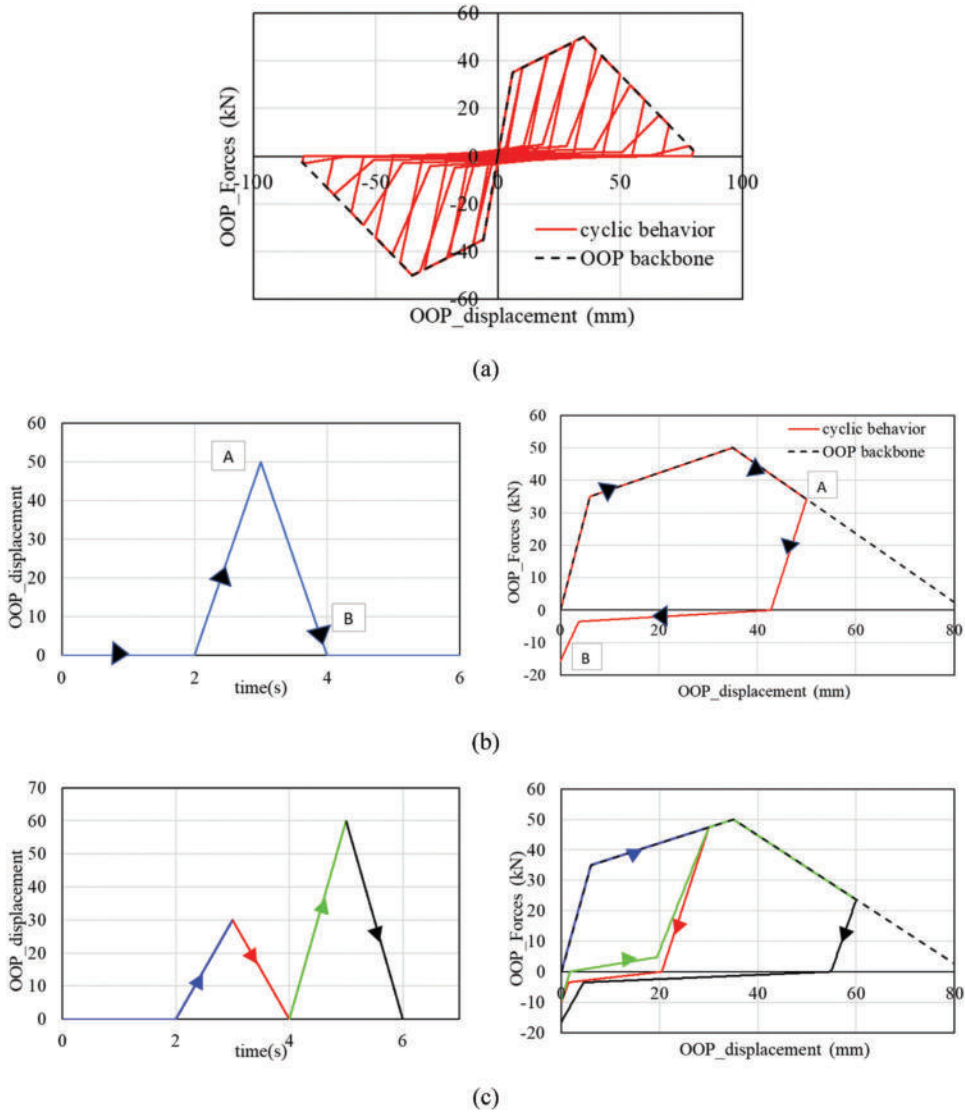


Figure 10. Cyclic behavior of the uniaxial hysteretic material used to describe the OOP behaviour of infills: (a) Full cyclic behavior; (b) Single loading / unloading cycle; (c) Loading / unloading / reloading cycle.

clarity, [Figs. 10\(b,c\)](#) show single loading/unloading/reloading cycles following different OOP displacement-time histories.

The OOP strength of the infills is reduced to account for the presence of the openings, according to the formulation proposed by Mays, Hetherington, and Rose (1998). Experimental IP/OOP curves are converted into building specific IP/OOP curves based on the infill’s cross-section area (for the IP behaviour) and infill’s length (for the OOP behaviour). [Figure 11](#) shows the OOP undamaged backbone curves of typical traditional infill (thick and thin leaf) and decoupled infill with INODIS, used for the numerical simulations.

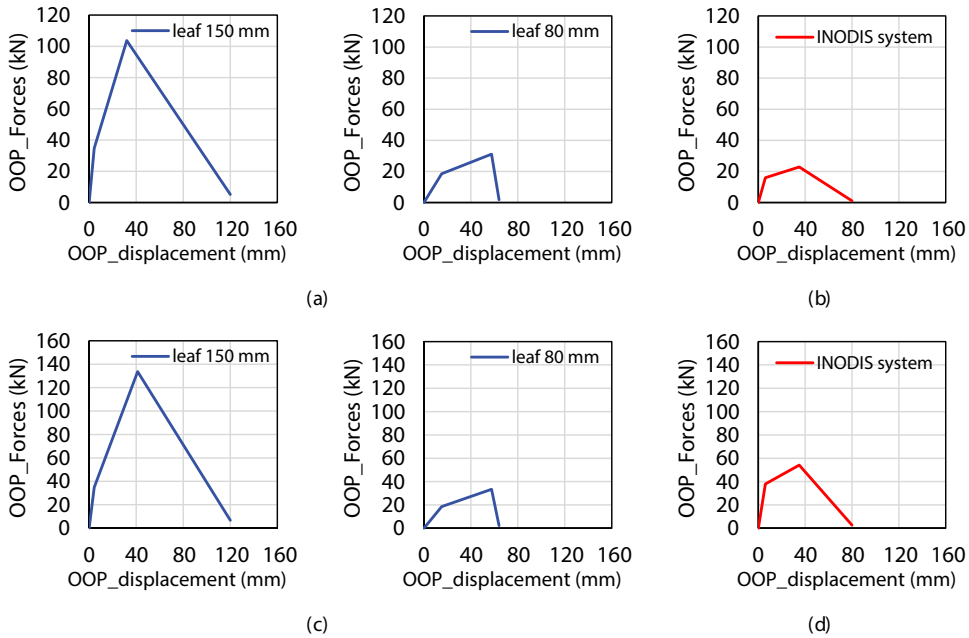


Figure 11. OOP undamaged backbone curves of traditional double-layer infills (leaf 150mm and leaf 80mm) and decoupled infills with INODIS system, with openings (a,b) and without openings (c,d).

Table 1. Fundamental periods of vibration.

	T_x (s)	T_y (s)
Bare frame (BF)	1.295	0.967
Infilled frame with traditional infills (IF)	0.605	0.573
Infilled frame with decoupled infills (IF-I)	1.203	0.912

4. Analysis Results

4.1. Modal Analysis

Modal analysis has been performed after the application of gravity loads. The fundamental periods of vibration of the building in the two orthogonal directions are reported in Table 1. Table 1 clearly points out that the presence of decoupled infills does not significantly affect the period of vibration of the bare RC frame. Traditional infills, instead, significantly increase the lateral stiffness of the building, thus strongly reducing its fundamental periods of vibration.

4.2. Pushover Analysis

Pushover analysis (POA) has been performed to derive the capacity curves of the case-study building and the displacement levels associated with some remarkable performance points, such as: (i) first yielding, (ii) attainment of peak strength and (iii) 15% reduction of the peak lateral strength. Both modal (M) and uniform (U) load patterns have been used in the two orthogonal directions (X and Z). Figure 12 shows the pushover curves derived from POA. The solid lines correspond to the pushover curves of the infilled frame while the dashed lines represent the contribution of the RC frame only. Frame only curves have been derived subtracting from the total base shear the contribution of the infill elements. Figure 12 clearly shows the stiffening contribution of traditional infills, especially in the short direction (no openings). The pushover curves of

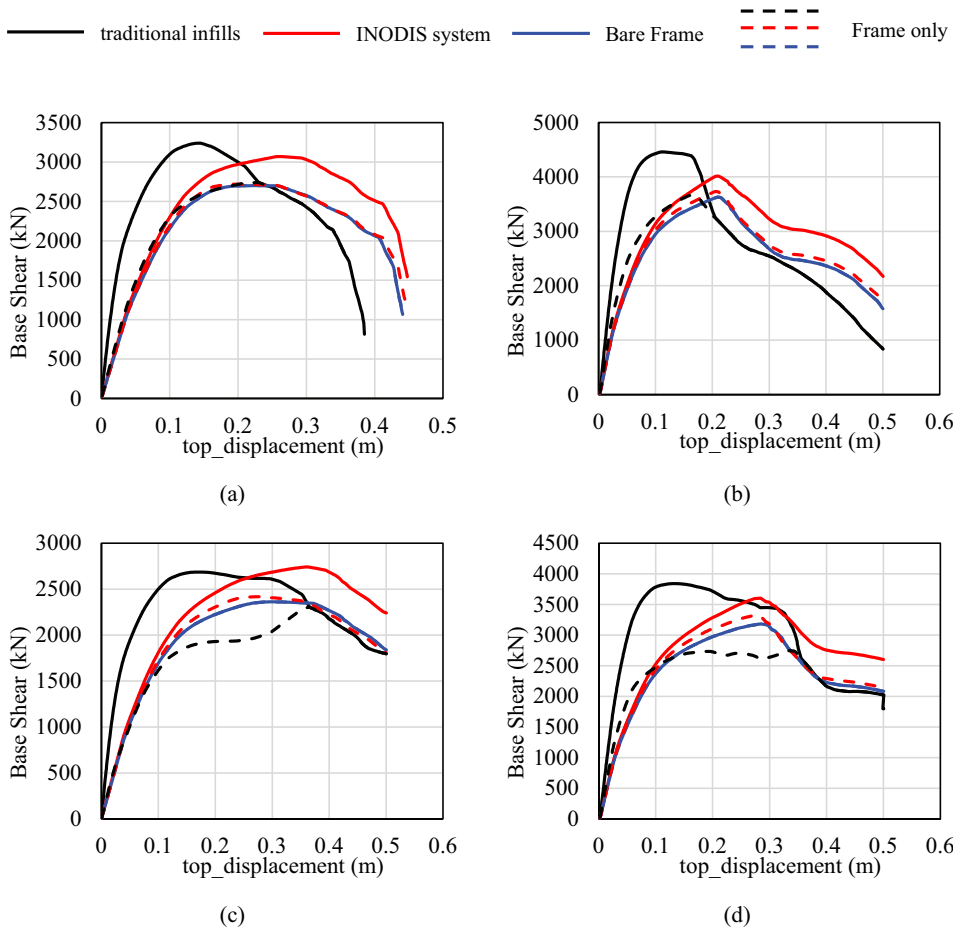


Figure 12. Pushover curves of the building: (a) Uniform force distribution along X-dir. And (b) Z-dir.; (c) Modal force distribution along X-dir. And (d) Z-dir.

the model with decoupled infills looks like those of the bare frame for the whole range of displacement. As expected, the pushover curves of the model with traditional infills tend to overlap the pushover curves of the bare frame for large displacements, due to the extensive damage of the masonry infills.

Figure 13 shows the drift profiles associated with first yielding, peak strength and 15% drop of lateral strength, respectively, for the model (a) with decoupled infills and (b) with traditional infills. It is worth noting the IDR demand distribution for the two building models: there is a higher IDR demand concentration with traditional infills than with INODIS, especially at lower seismic intensities (see first column in Fig. 13) before extensive damage develop in traditional infills at the highest seismic intensities (see last column of Fig. 13).

It is interesting to note that (see Fig. 13), for the building with decoupled infills, the maximum drift associated with the first yielding is lower than 0.5%, while the maximum drift at the peak force is around 2%. At 15% drop of the lateral global strength of the RC frame, the maximum drift exceeds 3% in the X-direction (long direction, with wide openings in the infills), and it is around 2.5% in the Z-direction (short direction, fully infilled without openings). This is in good agreement with the indications of (Rossetto and Elnashai 2003), who set around 3% maximum IDR the onset of extensive damage for older RC frame buildings with substandard seismic details. No shear failure due to the RC column/masonry infill interaction is observed.

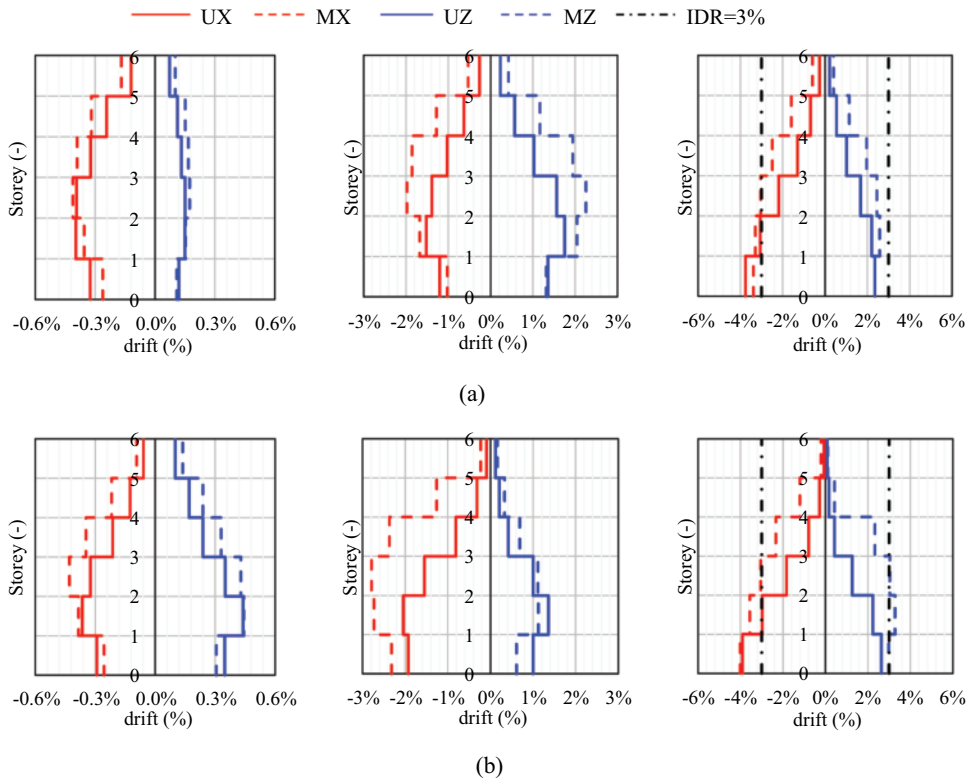


Figure 13. Drift profiles associated with first yielding peak strength and 15% drop of lateral strength respectively, for the model with decoupled infills (a) and with traditional infills (b).

4.3. Non-Linear response-Time History Analyses (NTHA)

Non-linear response-Time History Analyses (NTHA) have been performed to evaluate the seismic performance of the building for three different earthquake intensity levels (EQ-ILs), with return periods equal to 50 years, 500 years and 2500 years, respectively.

For each earthquake intensity level, NTHA have been performed using a set of 20 ground motion pairs selected and scaled by Ay, Fox, and Sullivan (2017), in such a way to be compatible with suitable Conditional Mean Spectra (CMS) (Baker 2011), derived considering an appropriate $M - R - \epsilon$ (magnitude – distance – epsilon) disaggregation and a suitable attenuation relationship for each building site.

Figure 14 shows the cyclic behaviour of a beam, a column, and a beam-column joint located at the 3rd storey of the building with decoupled infills during the 16th run at 50 yrs EQ-IL, 12th run at 500 yrs EQ-IL and 15th run at 2500 yrs EQ-IL, respectively. As can be seen, plastic deformations start to develop around 500 yrs EQ-IL. All RC elements experience extensive plastic deformations and degradation effects at the highest seismic intensity (2500 yrs EQ-IL).

Figure 15 and 16 show the interstorey drift profiles (IDR) derived from NTHA while increasing the earthquake intensity levels for the model with traditional infills and with decoupled infills, respectively. The number between brackets identifies the spectral acceleration at the conditioning period for each earthquake intensity level. Grey lines represent the maximum values recorded for the i -th run, while the black thick line indicates the average value over 20 ground motion pairs. As it can be seen, the IDR profiles feature a bulged shape with higher values at the mid-lower storeys of the building. The bulged shape becomes more pronounced as seismic intensity increases. This is due to the tapering of RC columns from second to third floor and then again from fourth to fifth floor. Consequently, also

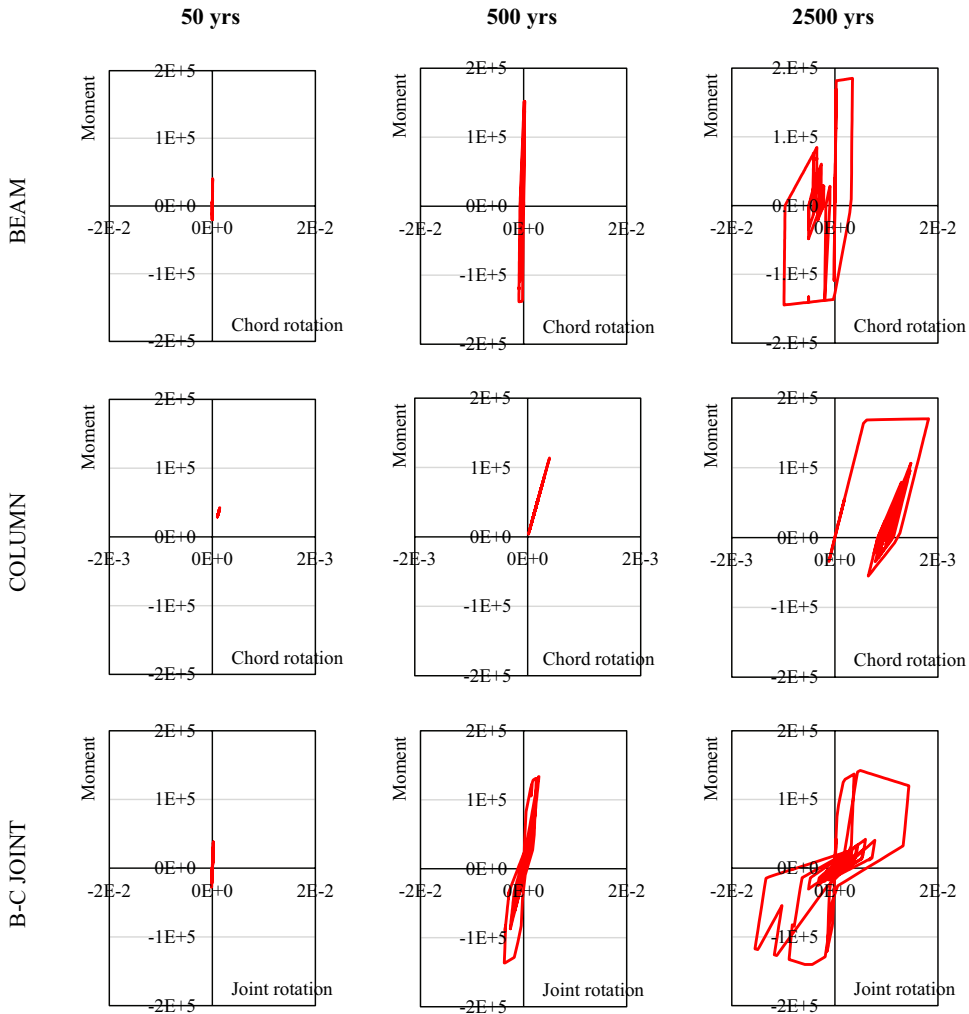


Figure 14. Cyclic behaviour of selected RC members located at the 3rd storey of the model with decoupled infills during run 16 at 50 yrs EQ-IL run 12 at 500 yrs EQ-IL and run 15 at 2500 yrs EQ-IL respectively.

the ductility demand tends to remain concentrated in the mid-lower storeys of the building, in accordance with what observed in Cardone et al. (2017).

Figure 17 compares the average maximum drift profiles obtained for each seismic intensity in the two directions. At low-to-medium seismic intensities (50–500 years return period, see Fig. 17(a,b)) the model with traditional infills features drift profiles a little lower than the model with decoupled infills, due to the significant stiffening effects of traditional infills (rigidly connected with the frame). At the highest seismic intensities (2500 years return period, see Fig. 17(c)), the maximum drifts experienced by the model with traditional infills are significantly higher than the model with decoupled infills, due to the extensive damage of traditional infills. Actually, the contribution of traditional infills to the frame lateral stiffness significantly decreases while increasing damage, because of two concurrent phenomena, i.e. the attainment of very large IDR, with consequent significant decrease in the IP response of the infill (displacement-dependent stiffness degradation) and IP degradation due to OOP damage (strength degradation due to IP/OOP interaction). Larger IDR for the model with traditional infills also implies larger inelastic demands in the RC members.

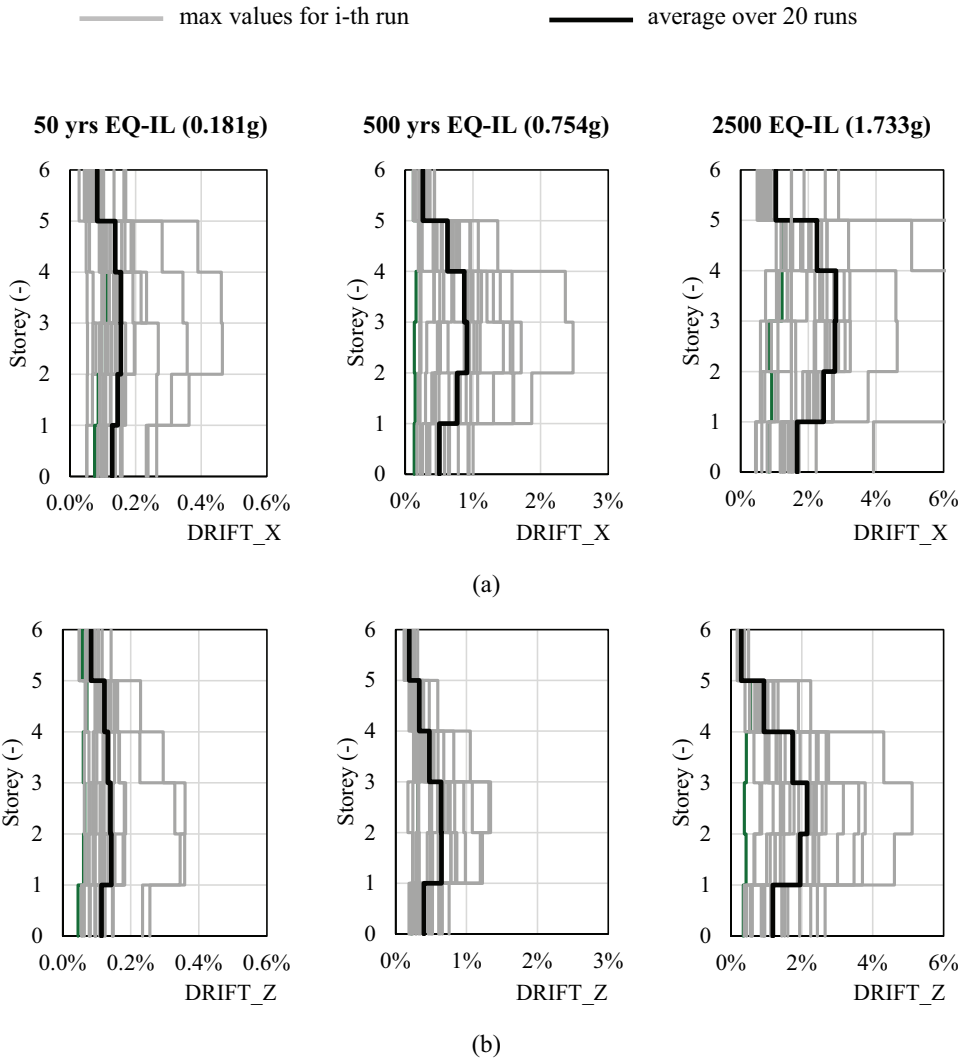


Figure 15. Drift profiles from NTHA: (a) X-dir. (long side); (b) Z-dir. (short side) of the model with traditional infills.

As a matter of fact, under strong earthquakes, the maximum seismic response of RC frames with traditional infills tends to progressively resemble that of a frame without infills (except for the upper storeys). On the other hand, the seismic behaviour of RC frames with decoupled infills is little affected by the lateral stiffness of the masonry walls and their response is almost the same as that of a bare frame at any seismic intensity. At the highest earthquake intensity levels, the shapes of the drift profiles of the building with traditional and decoupled infills are similar. However, traditional infills are severely damaged or destroyed, while decoupled infills remain almost undamaged.

Figures 18 and 19 compare the average values (out of 20 seismic record pairs) of the maximum floor acceleration and maximum infill OOP acceleration demand, along two verticals of the building located in the long (V1) and short (V2) direction, respectively. For the model with traditional infills (see Fig. 18), maximum storey and infill accelerations registered along the height of the building are of the same order of magnitude of $S_a(T^*)$ at low seismic intensities (50 yrs EQ-IL), while they result much lower at higher seismic intensities (500–2500 yrs EQ-ILs), due to the elongation of the fundamental period of vibration of the building following infill damage. For the model with decoupled infills, on the

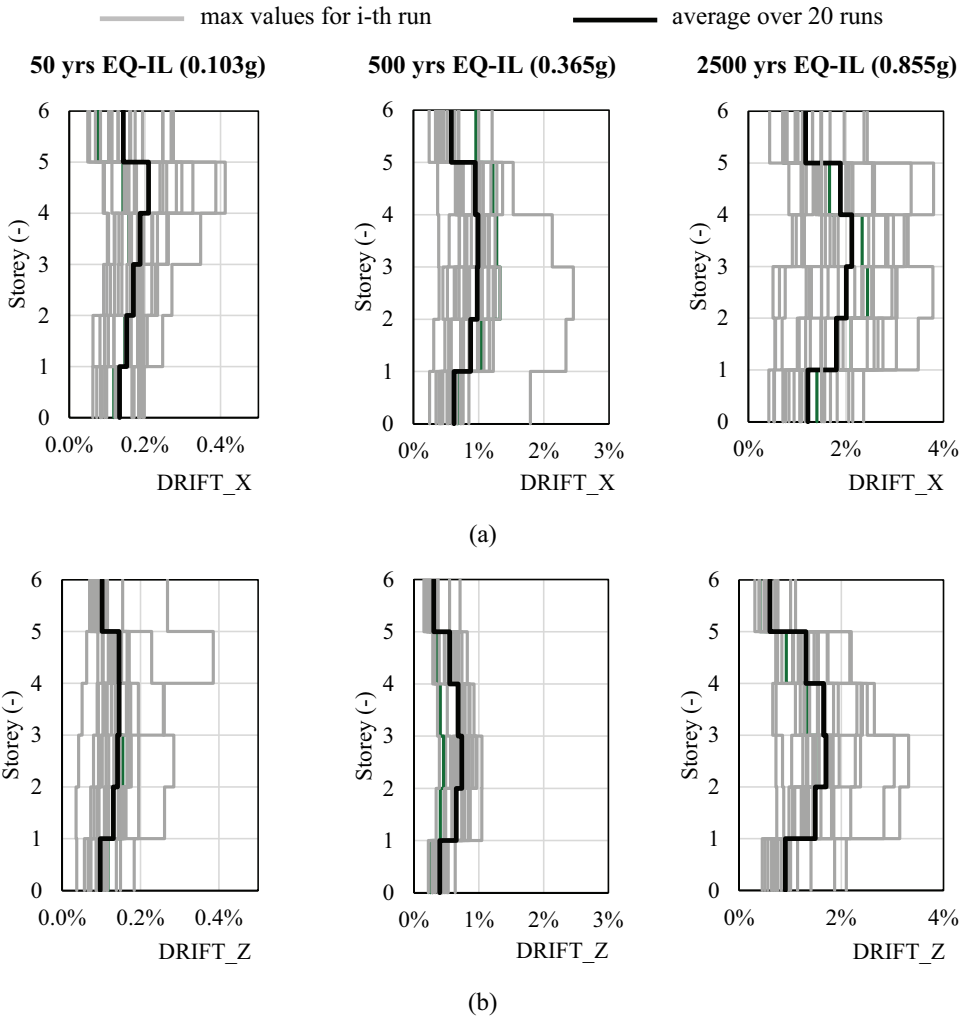


Figure 16. Drift profiles from NTHA: (a) X-dir. (long side); (b) Z-dir. (short side) of the model with decoupled infills.

contrary, maximum storey and infill accelerations registered along the height of the building are comparable to $S_a(T^*)$ at any seismic intensity, because decoupled infills do not suffer significant damage as seismic intensity increases. The acceleration amplification (with respect to the spectral value) observed in the mid-upper storeys of the model with decoupled infills is due to the tapering of the RC columns. Another interesting observation is that the maximum OOP acceleration demands are comparable to the corresponding mid-storey maximum floor accelerations, except for the ground level, where they are significantly higher. This was expected since the panels of the ground floor are connected directly to the foundation and therefore have a shorter period compared to those located on the upper storeys. Indeed, the model implemented implicitly addresses the topic of amplification of accelerations in nonstructural components depending on their period of vibration and location along the height of the building. The main aspects of the relationship between Peak Ground Acceleration (PGA), Peak Floor Acceleration (PFA) and Peak Spectral Acceleration (PSA) are discussed in detail in (Di Domenico et al. 2021) for bare RC frames and RC frames with and without masonry infills. The key role of the relationship between the higher-modes periods of the structure and the fundamental

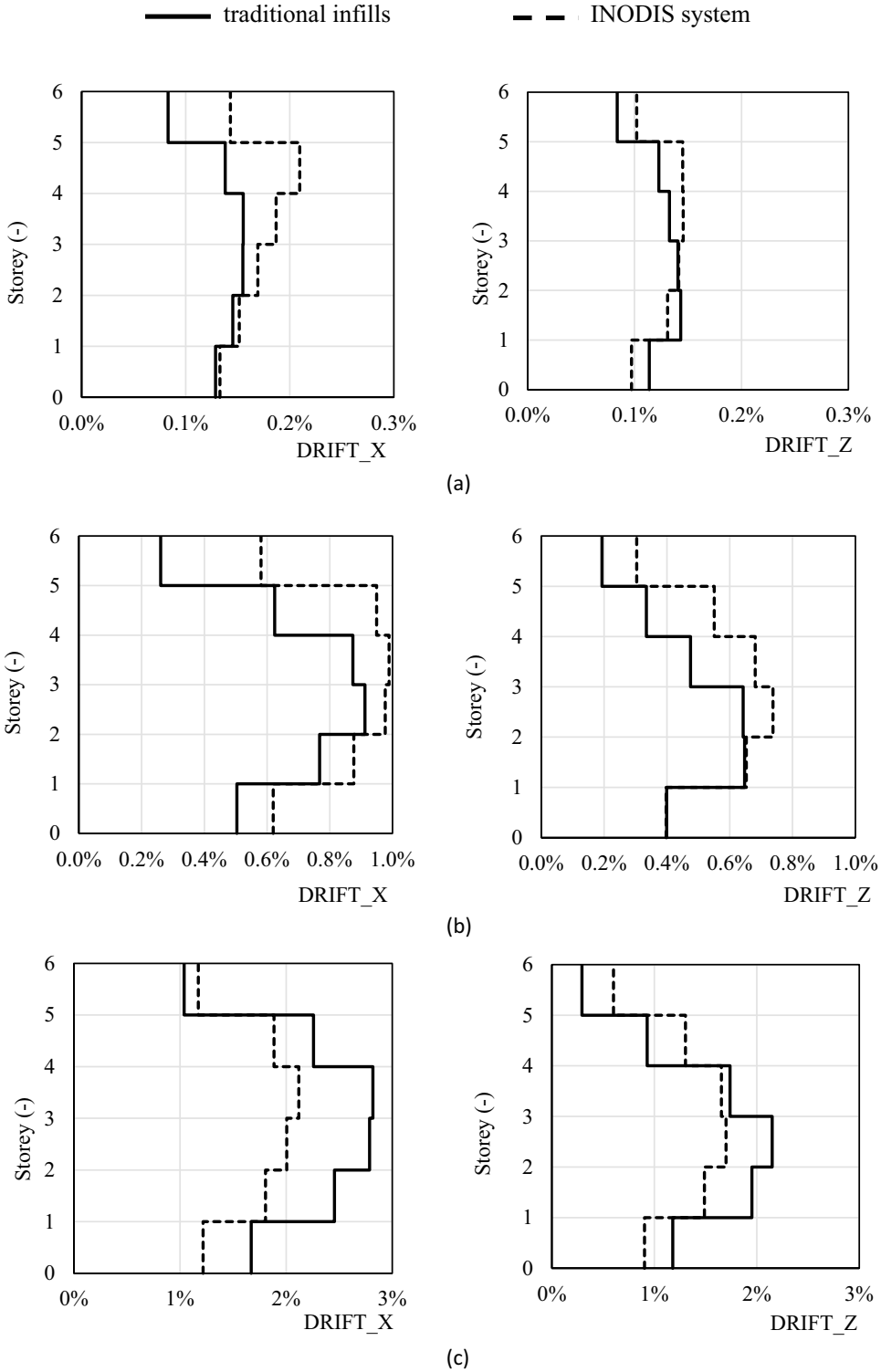


Figure 17. Comparison between average drift profiles in the two directions for different earthquake intensity levels with (a) 50 years, (b) 500 years and (c) 2500 years return period, respectively.

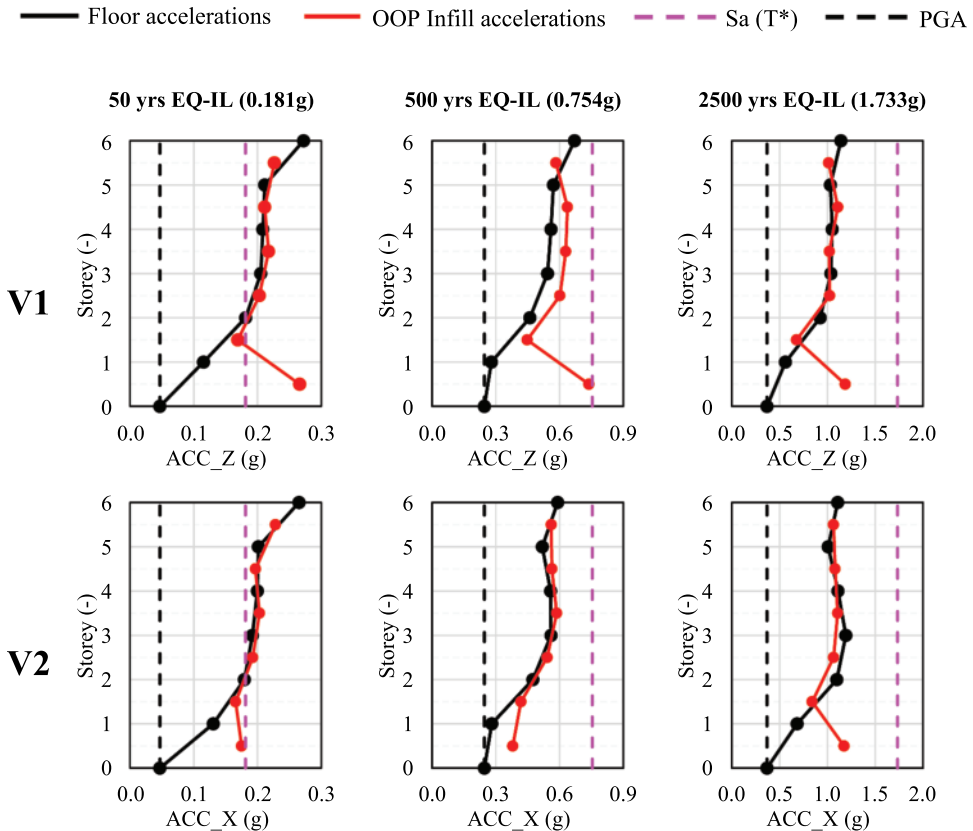


Figure 18. Comparison between maximum floor accelerations and maximum OOP infill accelerations for the model with traditional infills.

period of vibration of the non-structural components was experimentally demonstrated in (Dolce and Cardone 2003).

Figure 20 compares the average maximum storey accelerations (out of 20 accelerograms) recorded for each seismic intensity for the two models under consideration. Being more rigid, the models with traditional infills exhibit greater accelerations at low seismic intensities; the trend then changes passing to higher intensities, where the profiles become almost comparable, due to the progressive damage of the traditional infills.

Figure 21 shows the cyclic behaviour of a typical infill experiencing out-of-plane collapse. The infill is located at the first storey of the building. As a matter of fact, OOP collapse is mainly due to severe damage suffered in the IP direction. Indeed, the infill under consideration undergoes a maximum interstorey drift of about 2% and then collapses in the out-of-plane direction due to a maximum acceleration of 1.95 g. The OOP stiffness/strength degradation due to the high values of interstorey drifts is the main reason for the OOP collapse. This example clearly proves the effectiveness and importance of the algorithm implemented in Opensees in capturing the IP/OOP interaction of masonry infills during seismic events.

Figures 22 and 23 give an overview on the number of infills collapsed during each run at (a) 500 yrs EQ-IL and (b) 2500 yrs EQ-IL, respectively, for the model with decoupled infills (left) and the model with traditional infills (right). Each panel is divided in 20 rows, one for each seismic record pair.

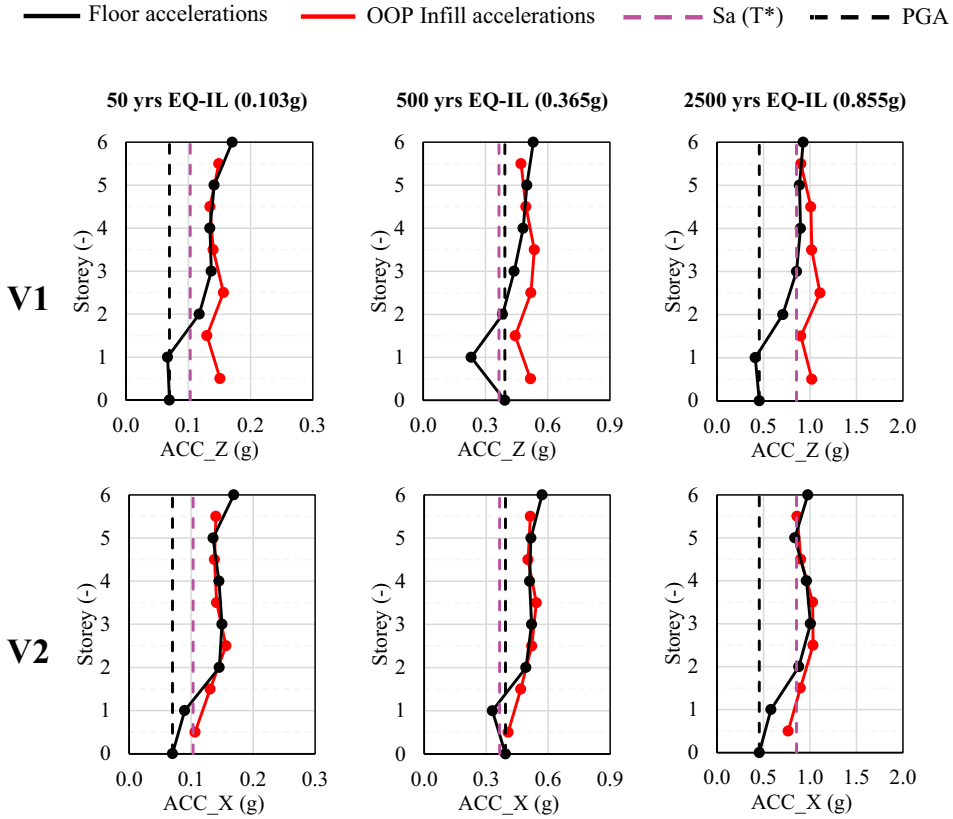


Figure 19. Comparison between maximum floor accelerations and maximum OOP infill accelerations for the model with decoupled infills.

Figures 22 and 23 confirm the great effectiveness of the INODIS system in protecting masonry infills from damage. As a matter of fact, for the model with decoupled infills, OOP collapse is recorded only for a few seismic events (2 out of 20) at 2500 yrs EQ-IL in the long direction (with openings), involving infills located at the lower storeys of the building. In addition, only a few infills undergo out-of-service conditions. It is worth mentioning that out-of-service conditions for decoupled infills have been deemed to occur for IDR greater than 3% due to significant damage in the adjacent RC structural elements. For the model with traditional infills, on the contrary, OOP collapse already occurs at 500 yrs EQ-IL. More importantly, most of traditional infills, along the entire height of the building (except the last storey), experience IP/OOP collapse at 2500 yrs EQ-IL, during almost all seismic records.

Figure 24 identifies some remarkable performance points related to different damage states of the infills: (i) IP/OOP first cracking (yellow), (ii) attainment of IP/OOP peak strength (orange), (iii) IP/OOP severe damage (light blue), conventionally assumed to occur when a drop of 20% in the peak force of the current (degraded) backbone curve is reached, (iv) OOP collapse (red) and (v) IP collapse (black). The aforesaid performance points provide the deformation capacity values for each masonry infill (infills with different aspect ratio feature different IDR capacity; infills with different mass feature different OOP displacement capacity). The only performance point for decoupled infills is represented by the onset of IP damage due to extensive damage in the adjacent RC frame (grey in Fig. 24). The

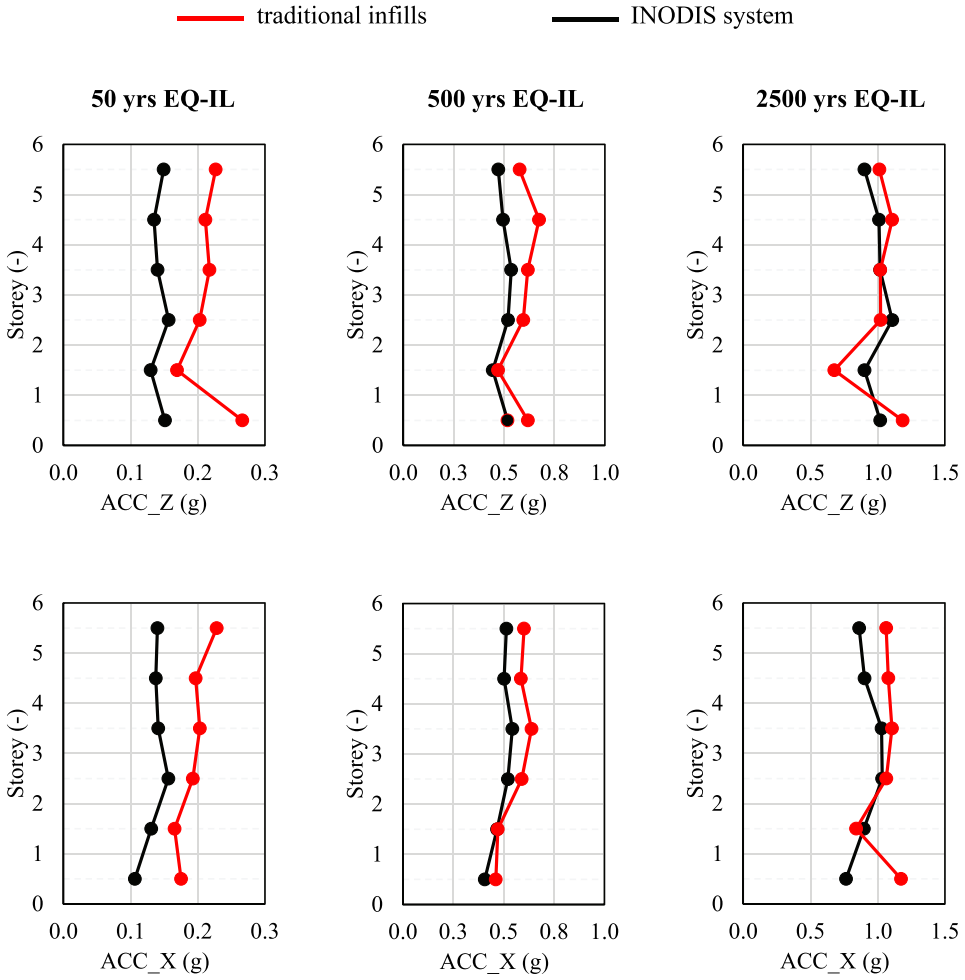


Figure 20. Comparison in terms of average (out of 20 accelerograms) maximum storey accelerations in the two directions, at different earthquake intensity levels.

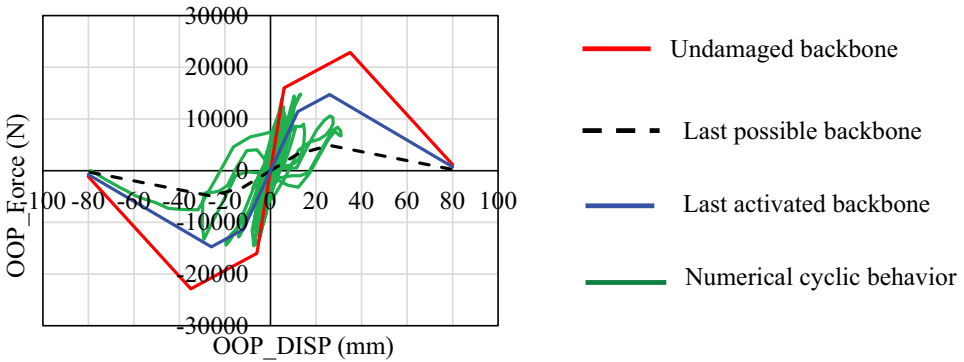


Figure 21. Cyclic behavior of a typical infill experiencing OOP collapse (1st storey infill; Run11 at 2500 yrs EQ-IL).

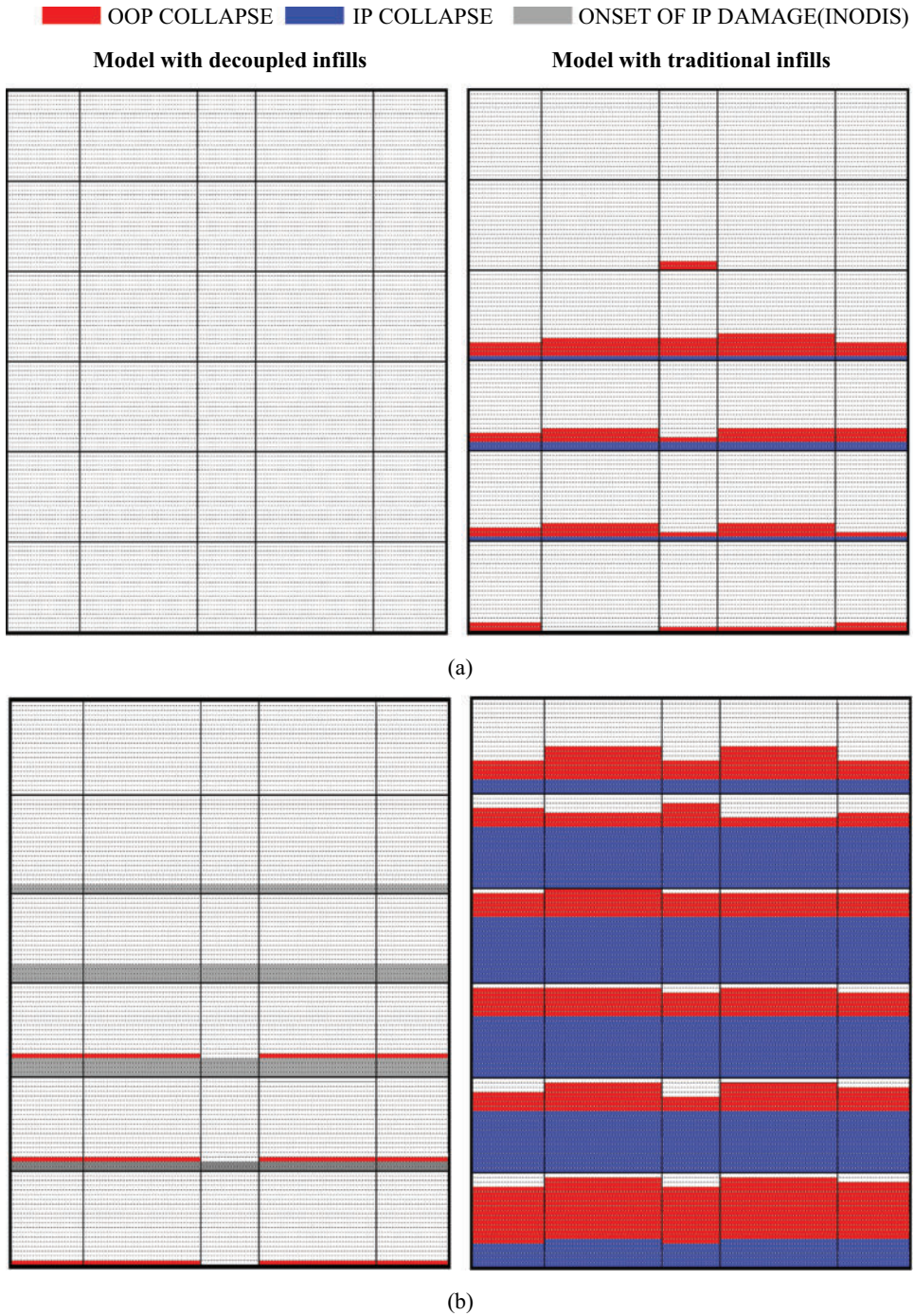
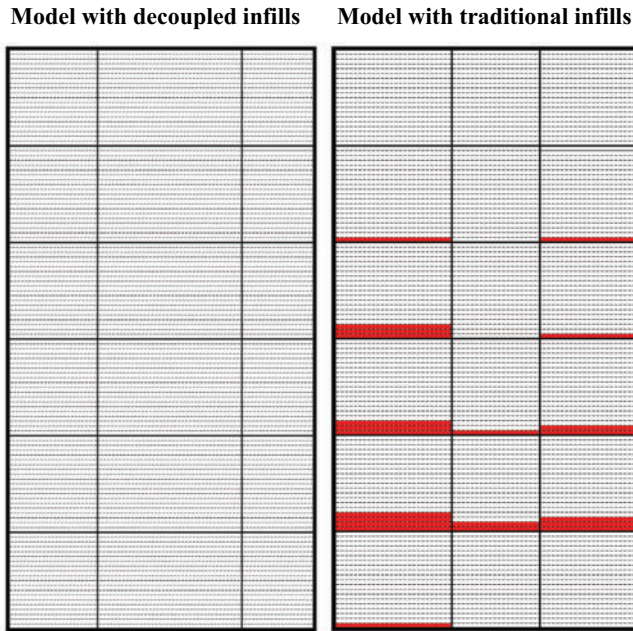


Figure 22. Number of infills experiencing IP/OOP collapse for each run at (a) 500 yrs EQ-IL and (b) 2500 yrs EQ-IL.

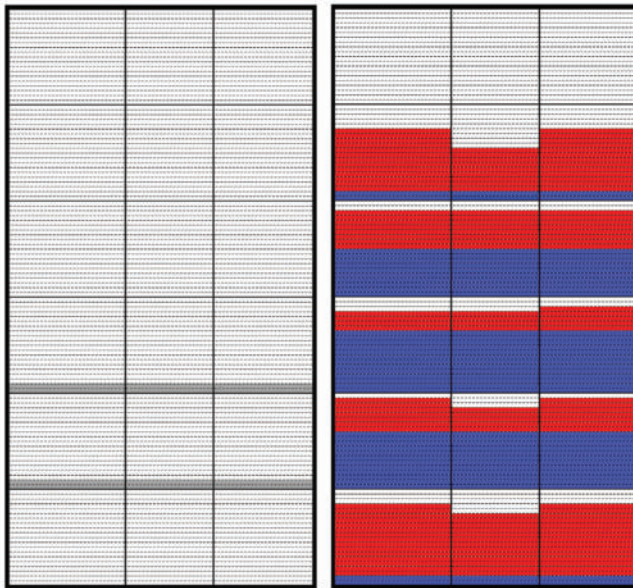
aforesaid performance points have been monitored during NTHA for each infill of the building. Outcomes are discussed in the following.

Tables 2 and 3 show the damage scenario of the building (related to masonry infills only) at a glance. The percentages reported in Tables 2 and 3 have been derived considering the average (out of

 OOP COLLAPSE  IP COLLAPSE  ONSET OF IP DAMAGE(INODIS)



(a)



(b)

Figure 23. Number of infills experiencing IP/OOP collapse for each run at (a) 500 yrs EQ-IL and (b) 2500 yrs EQ-IL.

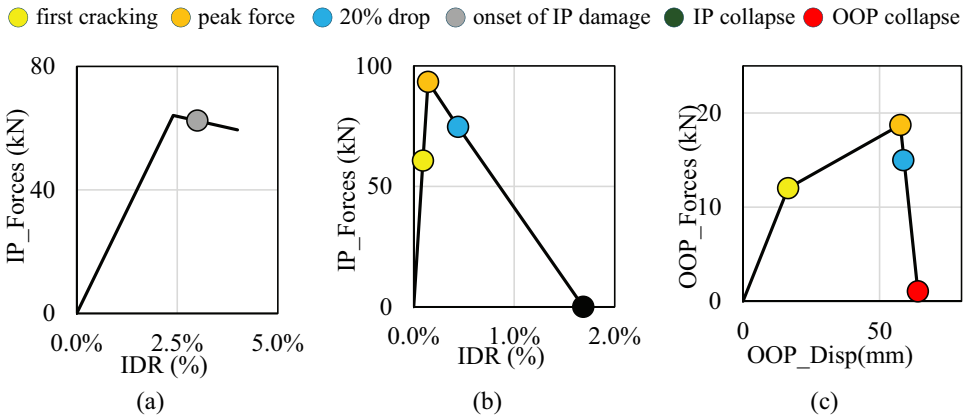


Figure 24. Performance points for (a) IP behaviour of decoupled infills, (b) IP behaviour of traditional and (c) OOP behaviour of both.

20 seismic record pairs) maximum IDR and OOP displacement demand recorded for each masonry infill. Damage states have been heuristically divided in “repairable” damage states (including IP/OOP first cracking and attainment of the IP/OOP peak force, see Fig. 24) and “not repairable” damage states (20% drop of the IP/OOP peak strength, IP/OOP collapse and out-of-service conditions due to extensive damage in the adjacent RC members for decoupled infills only, see Fig. 24). IP and OOP results are aggregated (without overlaps) in Table 4.

It is noted that at medium-high seismic intensities (500 yrs EQ-IL), more than 20% of traditional infills in the short direction (infills without openings) experienced not repairable damage; the percentage exceeds 70% in the long direction (infills with openings). At very high seismic intensities (2500 yrs EQ-IL), almost all traditional infills collapsed or suffered severe damage. On the other hand, less than 10% (5%) of decoupled infills experienced “not repairable” damage in the long (short) direction of the building, respectively, due to significant damage in the adjacent RC members.

To conclude, Fig. 25 points out that the use of decoupled infills can avoid any significant damage for rare earthquakes (500 years of return period) and considerably reduce (from around 85% to around 10% for the case study examined in this study) not-repairable damage of the infills for very rare earthquakes (2500 years return period).

5. Conclusions

The seismic performance of a RC frame building featuring, alternatively, traditional double layer infills and decoupled infills with the innovative INODIS system, have been compared.

Results of modal analysis clearly show that the periods of vibration of the RC frame building remain almost unchanged when decoupled infills are used. On the other hand, significantly higher values of lateral stiffness (compared to the bare frame) are achieved when traditional infills, rigidly connected to the surrounding RC frame, are used. Similar conclusions can be drawn comparing the capacity curves of the two building configurations. Indeed, the capacity curve of the model with decoupled infills looks like that of the bare frame over the whole displacement range. On the other hand, the capacity curve of the model with traditional infills results significantly stronger, compared to the bare frame, for small displacements while it tends to the bare frame curve for large displacements, due to the extensive damage of the masonry infills.

Table 3. Percentage of infills exceeding different levels of OOP damage (from first cracking to collapse) for the model with traditional infills and with decoupled infills, respectively.

	TRADITIONAL INFILL						INODIS SYSTEM								
	X-direction (long side)			Z-direction (short side)			X-direction (long side)			Z-direction (short side)					
	<i>repairable damage</i>	<i>not repairable damage</i>	<i>not repairable damage</i>	<i>repairable damage</i>	<i>not repairable damage</i>	<i>not repairable damage</i>	<i>repairable damage</i>	<i>not repairable damage</i>	<i>not repairable damage</i>	<i>repairable damage</i>	<i>not repairable damage</i>	<i>not repairable damage</i>			
	OOP peak force	OOP 20% drop	OOP collapse	OOP first crack	OOP peak force	OOP 20% drop	OOP collapse	OOP first crack	OOP peak force	OOP 20% drop	OOP collapse	OOP first crack	OOP peak force	OOP 20% drop	OOP collapse
500 yrs EQ-IL	10.6%	9.8%	9.8%	5.0%	4.7%	4.7%	2.2%	2.2%	—	—	—	—	—	—	—
2500 yrs EQ-IL	40.6%	32.0%	20.4%	46.8%	38.3%	33.5%	14.0%	14.0%	2.6%	2.6%	2.2%	—	—	—	—

Table 4. Percentages of infills experiencing repairable and non-repairable damage (figures obtained by aggregating IP and OOP damage without overlaps).

	TRADITIONAL INFILL				INODIS SYSTEM			
	X-direction (long side)		Z-direction (short side)		X-direction (long side)		Z-direction (short side)	
	REPAIRABLE DAMAGE	NOT REPAIRABLE DAMAGE	REPAIRABLE DAMAGE	NOT REPAIRABLE DAMAGE	REPAIRABLE DAMAGE	NOT REPAIRABLE DAMAGE	REPAIRABLE DAMAGE	NOT REPAIRABLE DAMAGE
<i>500 yrs EQ-IL</i>	27.5%	72.5%	64.0%	20.1%	3.1%	–	–	–
<i>2500 yrs EQ-IL</i>	7.8%	92.2%	21.0%	75.7%	19.4%	11.8%	2.5%	3.3%

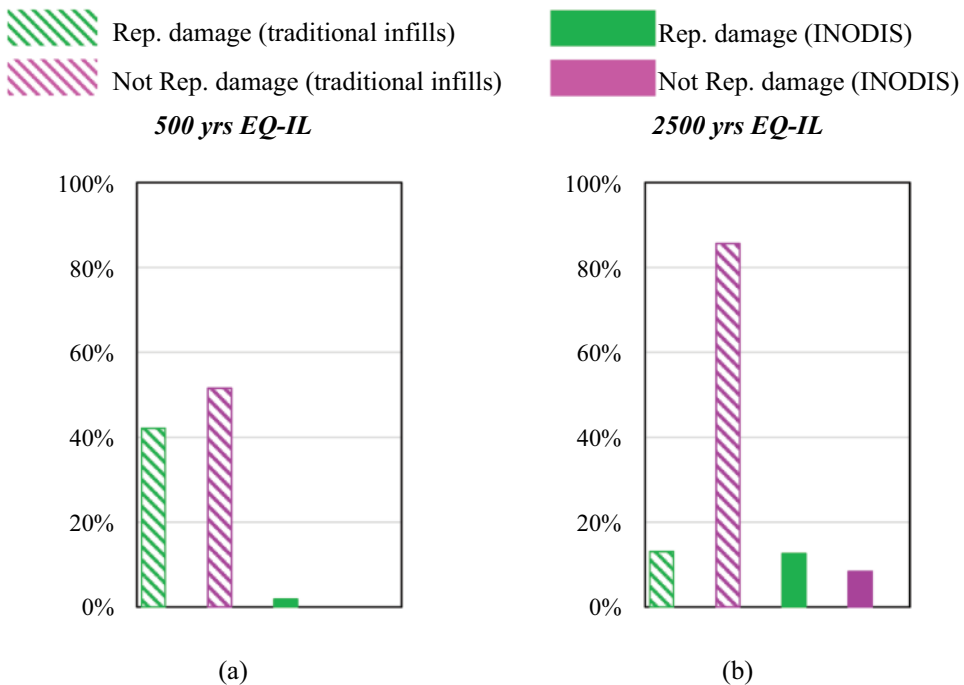


Figure 25. Total percentages of infills experiencing repairable and not-repairable damage (figures obtained by aggregating IP and OOP damage without overlaps).

Results from Nonlinear response-Time History analyses (NTHA) clearly show the great effectiveness of the INODIS system in limiting the extension and severity of damage in masonry infills up to very high seismic intensities. As a matter of fact, in the model with traditional infills more than 50% of infills would collapse or would be not repairable after an earthquake with 500 yrs return period while no damage would be observed in any infill, at the same seismic intensity, for the building with decoupled infills. Similarly, in the model with traditional infills more than 85% of infills would collapse or would be not repairable after an earthquake with 2500 yrs return period while only a few infills (around 10% of the total) should be replaced in the building with decoupled infills.

To conclude, based on the result of this preliminary study (which is limited to one case study, considering one traditional masonry infill typology only), the application of the INODIS system significantly improves the seismic performance of RC frame buildings. Reduced damage to non-structural elements may lead to great savings after an earthquake due to no repair costs and no interruptions of

activities. Obviously, further analyses (involving different RC buildings, infill types, seismic hazard conditions, etc.) are needed to draw more robust conclusions on the benefits of adopting the INODIS decoupling system in RC frame buildings.

Disclosure Statement

No potential conflict of interest was reported by the author(s).

Funding

The work was partly supported by DAAD (German Academic Exchange Service) through the scholarship # 91799375 within the 2021 Research Stays for University Academics and Scientists funding program.

ORCID

Marinković Marko  <http://orcid.org/0000-0001-6642-8403>

Data Availability Statement

All numerical results of this study are available from the corresponding author upon reasonable request.

References

- Akhoundi, F., G. Vasconcelos, P. Lourenço, L. M. Silva, F. Cunha, and R. Figueiro. 2018. "In-Plane Behavior of Cavity Masonry Infills and Strengthening with Textile Reinforced Mortar." *Engineering Structures* 156:145–160. <https://doi.org/10.1016/j.engstruct.2017.11.002>.
- Aslani, H., and E. Miranda. (2005). *Probabilistic Earthquake Loss Estimation and Loss Disaggregation in Buildings*. Report No. 157, The John A. Stanford, CA, USA: Blume Earthquake Engineering Center, Department of Civil and Environmental Engineering, Stanford University. 460.
- Asteris, P. G., C. C. Repapis, A. K. Tsaris, F. Di Trapani, and L. Cavaleri. 2015. "Parameters Affecting the Fundamental Period of Infilled RC Frame Structures." *Earthquakes & Structures* 9 (5): 999–1028. <https://doi.org/10.12989/eas.2015.9.5.999>.
- Ay, B. Ö., M. J. Fox, and T. J. Sullivan. 2017. "Technical Note: Practical Challenges Facing the Selection of Conditional Spectrum Compatible Accelerograms." *Journal of Earthquake Engineering* 21 (1): 169–180. <https://doi.org/10.1080/13632469.2016.1157527>.
- Baker, J. W. 2011. "Conditional Mean Spectrum: Tool for Ground Motion Selection." *Journal of Structural Engineering* 137 (3): 322–331. [https://doi.org/10.1061/\(ASCE\)ST.1943-541X.0000215](https://doi.org/10.1061/(ASCE)ST.1943-541X.0000215).
- Braga, F., V. Manfredi, A. Masi, A. Salvatori, and M. Vona. 2011. "Performance of Non-Structural Elements in RC Buildings During the L'Aquila, 2009 Earthquake." *Bulletin of Earthquake Engineering* 9 (1): 307–324. <https://doi.org/10.1007/s10518-010-9205-7>.
- Calvi, G. M., and D. Bolognini. 2001. "Seismic Response of Reinforced Concrete Frames Infilled with Weakly Reinforced Masonry Panels." *Journal of Earthquake Engineering* 5 (2): 153–185. <https://doi.org/10.1080/13632460109350390>.
- Cardone, D., and G. Perrone. 2017. "Damage and Loss Assessment of Pre-70 RC Frame Buildings with FEMA P-58." *Journal of Earthquake Engineering* 21 (1): 23–61. <https://doi.org/10.1080/13632469.2016.1149893>.
- Cardone, D., T. J. Sullivan, G. Gesualdi, and G. Perrone. 2017. "Simplified Estimation of the Expected Annual Loss of Reinforced Concrete Buildings." *Earthquake Engineering & Structural Dynamics* 46 (12): 2009–2032. <https://doi.org/10.1002/eqe.2893>.
- Da Porto, F., G. Guidi, M. Dalla Benetta, and N. Verlato. 2013. "Combined In-Plane/out-Of-Plane Experimental Behaviour of Reinforced and Strengthened Infill Masonry Walls." *12th Canadian masonry symposium*, Vancouver, British Columbia, Canada, 2–5. June.
- Decanini, L., L. Liberatore, and F. Mollaioli. 2014. "Strength and Stiffness Reduction Factors for Infilled Frames with Openings." *Earthquake Engineering and Engineering Vibration* 13 (3): 437–454. September, 2014. <https://doi.org/10.1007/s11803-014-0254-9>.
- Decanini, L., F. Mollaioli, A. Mura, and R. Saragoni. 2004. "Seismic Performance of Masonry Infilled R/C Frames." Proceedings on 13th WCEE, Paper 165, Vancouver, B.C. Canada, Aug 1–6.

- Del Gaudio, C., M. T. De Risi, and G. M. Verderame. 2021. "Seismic Loss Prediction for Infilled RC Buildings via Simplified Analytical Method." *Journal of Earthquake Engineering* 26 (11): 5477–5510. <https://doi.org/10.1080/13632469.2021.1875940>.
- Di Domenico, M., M. T. De Risi, V. Manfredi, M. Terrenzi, G. Camata, F. Mollaioli, F. Noto, et al. 2022. "Modelling and Seismic Response Analysis of Italian Pre-Code and Low-Code Reinforced Concrete Buildings. Part II: Infilled Frames." *Journal of Earthquake Engineering* 27 (6): 1534–1564. <https://doi.org/10.1080/13632469.2022.2086189>.
- Di Domenico, M., P. Ricci, and G. M. Verderame. 2021. "Floor Spectra for Bare and Infilled Reinforced Concrete Frames Designed According to Eurocodes." *Earthquake Engineering & Structural Dynamics* 50 (13): 3577–3601. <https://doi.org/10.1002/eqe.3523>.
- Di Trapani, F., V. Bolis, F. Basone, and M. Preti. 2020. "Seismic Reliability and Loss Assessment of RC Frame Structures with Traditional and Innovative Masonry Infills." *Engineering Structures* 208:110306. <https://doi.org/10.1016/j.engstruct.2020.110306>.
- DM 19/06/1984. 1984. *Norme tecniche relative alle costruzioni sismiche*. Gazzetta Ufficiale n. 208 del 30 luglio 1984. in Italian.
- DM 24/01/1986. 1986. *Norme tecniche relative alle costruzioni antisismiche*. Gazzetta Ufficiale n. 108 del 12 maggio 1986. in Italian.
- Dolce, M., and D. Cardone. 2003. "Seismic Protection of Light Secondary Systems Through Different Base Isolation Systems." *Journal of Earthquake Engineering* 7 (2): 223–250. <https://doi.org/10.1080/13632460309350447>.
- Gesualdi, G., L. R. S. Viggiani, and D. Cardone. 2020. "Seismic Performance of RC Frame Buildings Accounting for the Out-Of-Plane Behavior of Masonry Infills." *Bulletin of Earthquake Engineering* 18 (11): 5343–5381. <https://doi.org/10.1007/s10518-020-00904-1>.
- Hak, S., P. Morandi, and G. Magenes. 2017. "Predictio—Of Inter—Storey Drifts for Regular RC Structures with Masonry Infills Based on Bare Frame Modelling." *Bulletin of Earthquake Engi—Ering* 16 (1): 397–425. <https://doi.org/10.1007/s10518-017-0210-y>.
- Hermanns, L., A. Fraile, E. Alarcón, and R. Álvarez. 2014. "Performance of Buildings with Masonry Infill Walls During the 2011 Lorca Earthquake." *Bulletin of Earthquake Engineering* 12 (5): 1977–1997. <https://doi.org/10.1007/s10518-013-9499-3>.
- Huang, W., X. Niu, C. Zhang, B. Ling, S. Wu, and D. X. Liang Z. 2024. "Experimental and Analytical Studies of Infill Wall with Sliding Joints Considering a Door Opening." *Earthquake Engineering & Structural Dynamics* 53 (6): 2162–2184. <https://doi.org/10.1002/eqe.4108>.
- Ibarra, L. F., and H. Krawinkler. 2005. "Global Collapse of Frame Structures under Seismic Excitations." In *Rep. No. TB*, Vol. 152. The John A. Blume Earthquake Engineering Center, Dept. of Civil and Environmental Engineering, Stanford University.
- Ibarra, L. F., R. A. Medina, and H. Krawinkler. 2005. "Hysteretic Models That Incorporate Strength and Stiffness Deterioration." *Earthquake Engineering & Structural Dynamics* 34 (12): 1489–1511. <https://doi.org/10.1002/eqe.495>.
- Marinković, M., and C. Butenweg. 2019. "Innovative Decoupling System for the Seismic Protection of Masonry Infill Walls in Reinforced Concrete Frames." *Engineering Structures* 197:109435. <https://doi.org/10.1016/j.engstruct.2019.109435>.
- Marinković, M., and C. Butenweg. 2022. "Numerical Analysis of the In-Plane Behaviour of Decoupled Masonry Infilled RC Frames." *Engineering Structures* 272:114959. <https://doi.org/10.1016/j.engstruct.2022.114959>.
- Marinković, M., M. Baballëku, B. Isufi, N. Blagojević, I. Milićević, and S. Brzev. 2022. "Performance of RC Cast-In-Place Buildings During the November 26, 2019 Albania Earthquake." *Bulletin of Earthquake Engineering* 5481–5482. <https://doi.org/10.1007/s10518-022-01439-3>.
- Mays, G. C., J. G. Hetherington, and T. A. Rose. 1998. "Resistance-Deflection Functions for Concrete Wall Panels with Openings." *Journal of Structural Engineering* 124 (5): 579–587.
- McKenna, F. 2011. "OpenSees: A Framework for Earthquake Engineering Simulation." *Computing in Science & Engineering* 13 (4): 58–66. <https://doi.org/10.1109/MCSE.2011.66>.
- Milanesi, R. R., P. Morandi, and G. Magenes. 2018. "Local Effects on RC Frames In-Duced by AAC Masonry Infills Through FEM Simulation of In-Plane Tests." *Bulletin of Earthquake Engineering* 16 (9): 1–28. <https://doi.org/10.1007/s10518-018-0353-5>.
- Morandi, P., R. R. Milanesi, and G. Magenes. 2018. "Innovative Solution for Seismic-Resistant Masonry Infills with Sliding Joints: In-Plane Experimental Performance." *Engineering Structures* 176:719–733. <https://doi.org/10.1016/j.engstruct.2018.09.018>.
- Mucedero, G., D. Perrone, and R. Monteiro. 2022. "Infill Variability and Modelling Uncertainty Implications on the Seismic Loss Assessment of an Existing RC Italian School Building." *Applied Sciences* 12 (23): 12002. <https://doi.org/10.3390/app122312002>.
- Mucedero, G., D. Perrone, and R. Monteiro. 2023. "Seismic Risk Assessment of Masonry-Infilled RC Building Portfolios: Impact of Variability in the Infill Properties." *Bulletin of Earthquake Engineering* 21 (2): 957–995. <https://doi.org/10.1007/s10518-022-01563-0>.

- Noh, N. M., L. Liberatore, F. Mollaioli, and S. Solomon Tesfamariam. 2017. "Modelling of Masonry Infilled RC Frames Subjected to Cyclic Loads: State of the Art Review and Modelling with OpenSees." 150:599–621. <https://doi.org/10.1016/j.engstruct.2017.07.002>
- Perrone, D., P. M. Calvi, R. Nascimbene, E. C. Fischer, and G. Magliulo. 2019. "Seismic Performance of Non-Structural Elements During the 2016 Central Italy Earthquake." *Bulletin of Earthquake Engineering* 17 (10): 5655–5677. <https://doi.org/10.1007/s10518-018-0361-5>.
- Preti, M., and V. Bolis. 2017. "Masonry Infill Construction and Retrofit Technique for the Infill-Frame Interaction Mitigation: Test Results." *Engineering Structures* 132:597–608. <https://doi.org/10.1016/j.engstruct.2016.11.053>.
- Priestley, M. J. 1985. "Seismic Behaviour of Unreinforced Masonry Walls, Bull." *Bulletin of the New Zealand Society for Earthquake Engineering* 18 (2): 191–205. 18. <https://doi.org/10.5459/bnzsee.18.2.191-205>.
- Ricci, P., M. Di Domenico, and G. M. Verderame. 2018a. "Experimental Investigation of the Influence of Slenderness Ratio and of the In-Plane/out-Of-Plane Interaction on the Out-Of-Plane Strength of URM Infill Walls." *Construction and Building Materials* 191:507–522. <https://doi.org/10.1016/j.conbuildmat.2018.10.011>.
- Ricci, P., M. Di Domenico, and G. M. Verderame. 2018b. "Empirical-Based Out-Of-Plane URM Infill Wall Model Accounting for the Interaction with In-Plane Demand." *Earthquake Engineering & Structural Dynamics* 47 (3): 802–827. <https://doi.org/10.1002/eqe.2992>.
- Ricci, P., V. Manfredi, F. Noto, M. Terrenzi, M. T. De Risi, M. Di Domenico, G. Camata, et al. 2019. "RINTC-E: Towards Seismic Risk Assessment of Existing Residential Reinforced Concrete Buildings in Italy." *Proceedings of the 7th 560 International Conference on Computational Methods in Structural Dynamics and Earthquake Engineering (COMPdyn 2019)*, 554–576. Crete, Greece. <https://doi.org/10.7712/120119.6939.20040>.
- Ricci, P., V. Manfredi, F. Noto, M. Terrenzi, C. Petrone, F. Celano, M. T. De Risi, et al. 2018. "Modeling and Seismic Response Analysis of Italian Code-Conforming Reinforced Concrete Buildings." *Journal of Earthquake Engineering* 22 (NO.S2): 105–139. <https://doi.org/10.1080/13632469.2018.1527733>.
- Ricci, P., G. M. Verderame, and G. Manfredi. 2011. "Analytical Investigation of Elastic Period of Infilled RC Mrbuildings." *Engineering Structures* 33 (2): 308–319. <https://doi.org/10.1016/j.engstruct.2010.10.009>.
- Rossetto, T., and A. Elnashai. 2003. "Derivation of Vulnerability Functions for European-Type RC Structures Based on Observational Data." *Engineering Structures* 25 (10): 1241–1263. [https://doi.org/10.1016/S0141-0296\(03\)00060-9](https://doi.org/10.1016/S0141-0296(03)00060-9).
- Rossi, A., P. Morandi, and G. Magenes. 2021. "A Novel Approach for the Evaluation of the Economical Losses Due to Seismic Actions on RC Buildings with Masonry Infills." *Soil Dynamics and Earthquake Engineering* 145:106722. <https://doi.org/10.1016/j.soildyn.2021.106722>.
- Sassun, K., T. J. Sullivan, P. Morandi, and D. Cardone. 2016. "Characterising the In-Plane Seismic Performance of Infill Masonry." *Bull N Z Soc Earthq Eng* 49 (1): 98–115. <https://doi.org/10.5459/bnzsee.49.1.98-115>.
- Taghavi, S., and E. Miranda. 2002. "Seismic Performance and Loss Assesment of Nonstructural Building Components." *Proceeding 7th National Conference on Earthquake Engineering*, Boston, Massachusetts, 21–25.
- Tasligedik, A. S. 2014. *Damage Mitigation Strategies for Non-Structural Infill Walls*. Civil and Natural Resources Engineering Department. [PhD thesis].
- Valluzzi, M. R., F. Da Porto, E. Garbin, and M. Panizza. 2014. "Out-Of-Plane Behaviour of Infill Masonry Panels Strengthened with Composite Materials." *Materials and Structures* 47 (12): 2131–2145. <https://doi.org/10.1617/s11527-014-0384-6>.
- Verlato, N., G. Guidi, F. da Porto, and C. Modena. (2016). Innovative Systems for Masonry Infill Walls Based on the Use of Deformable Joints: Combined In-Plane/out-Of-Plane Tests. *Proceedings of the 16th International Brick and Block Masonry Conference*, Padova, Italy.
- Villaverde, R. 1997. "Method to Improve Seismic Provisions for Nonstructural Components in Buildings." *Journal of Structural Engineering* 123 (4): 432–439. [https://doi.org/10.1061/\(ASCE\)0733-9445\(1997\)123:4\(432\)](https://doi.org/10.1061/(ASCE)0733-9445(1997)123:4(432)).
- Vintzileou, E., C. E. Adami, and V. Palieraki. 2016. "In-Plane and Out-Of-Plane Response of a Masonry Infill Divided into Smaller WalleTTes." *Proceedings of the 16th International Brick and Block Masonry Conference (IBMAC 2016)*, Padova, Italy.
- Zhang, C., T. Yu, Z. Chen, W. Huang, S. Zhang, Y. Zhou, L. Dehui, and Z. Lin. 2022. "Seismic Behavior of Novel Low-Damage Precast Infill Walls with Sliding Joints for Reinforced Concrete Frame." *Earthquake Engineering & Structural Dynamics* 51 (15): 3730–3754. <https://doi.org/10.1002/eqe.3746>.